

**KERNFORSCHUNGSZENTRUM
KARLSRUHE**

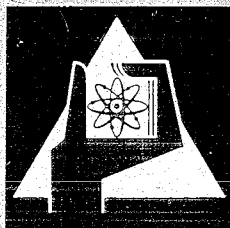
June 1970

KFK 1176

Institut für Angewandte Reaktorphysik
Institut für Neutronenphysik und Reaktortechnik
Projekt Schneller Brüter

A Fast Reactor Lattice Experiment for Investigation of k_{∞}
and Reaction Rate Ratios in SNEAK, Assembly 5

Compiled by
K. Böhnelt, H. Meister



GESELLSCHAFT FÜR KERNFORSCHUNG M. B. H.

KARLSRUHE



KERNFORSCHUNGSZENTRUM KARLSRUHE

Juni 1970

KFK-1176

Institut für Angewandte Reaktorphysik
Institut für Neutronenphysik und Reaktortechnik
Projekt Schneller Brüter

A Fast Reactor Lattice Experiment for Investigation of k_{∞}
and Reaction Rate Ratios in SNEAK, Assembly 5 +)

by

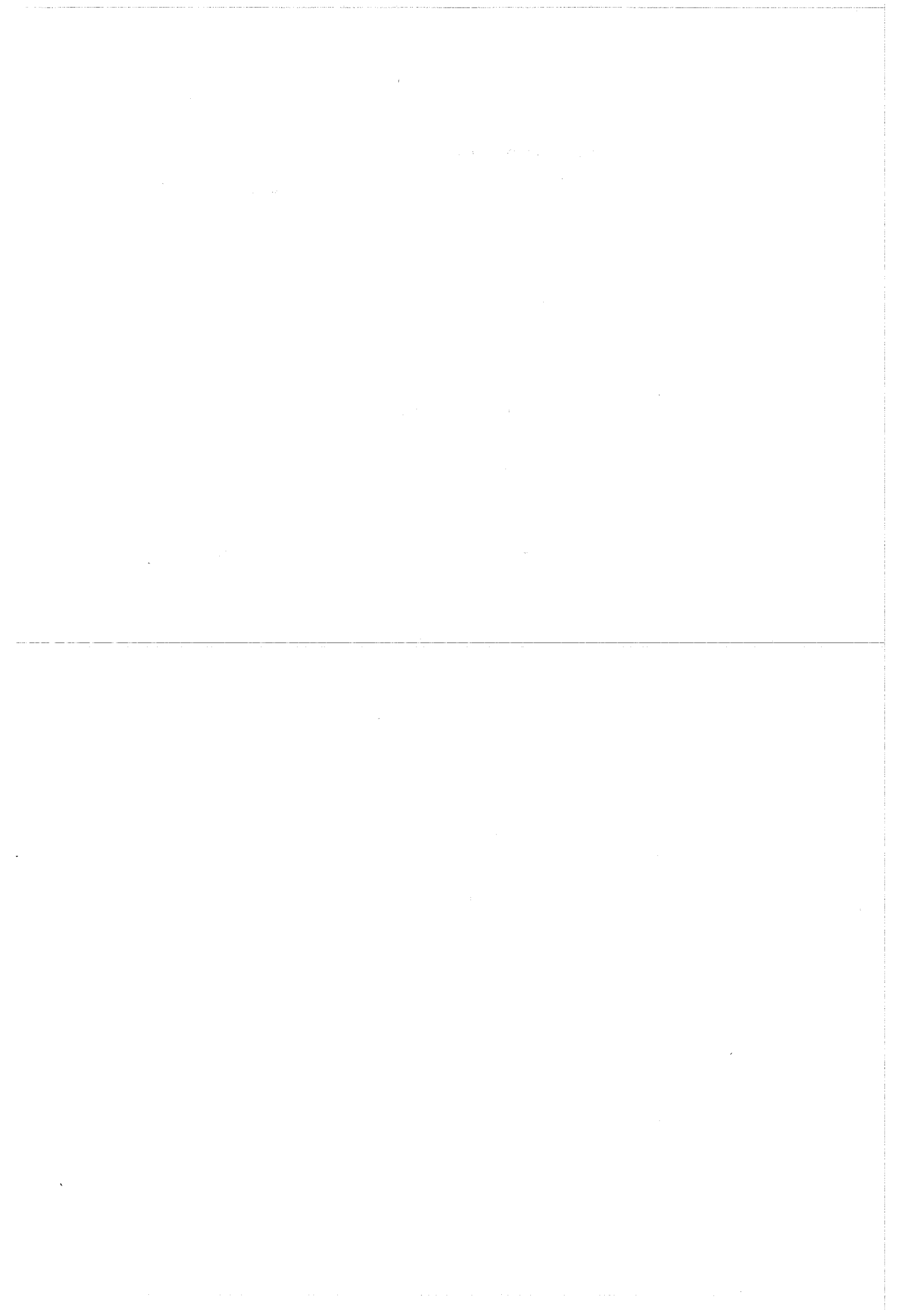
R.Böhme, K.Böhnel, R.Boix-Amat¹⁾, R.Eberle, E.Korthaus, D.Kuhn
H.Küsters, H.Meister, W.J.Oosterkamp, H.Seufert, and H.Werle.

compiled by

K. Böhnel and H. Meister

- +) Paper presented to the IAEA Meeting of Specialists on the Value of Plutonium Alpha, Winfrith, UK, June 30 - Juli 1, 1969.
- 1) On leave from Comisión Nacional de Energía Atómica, Buenos Aires, Argentina.

Gesellschaft für Kernforschung mbH, Karlsruhe



Abstract

A fast reactor lattice experiment was carried out in the zero-power facility SNEAK, assembly 5, to determine k_{∞} and reaction rate ratios. The assembly consists of a central test zone surrounded by axial and radial driver regions. The test zone contains platelets of PuO_2/UO_2 mixed oxide, depleted and natural uranium metal, and graphite as a moderating material. Its composition was chosen to render a k_{∞} close to unity.

The k_{∞} -values of systems with different C/ U^{238} -ratio were determined by voiding a central region of the test zone and measuring the associated reactivity change. Fission rates of U^{235} and U^{238} inside the lattice cell were measured with solid state track detectors, the U^{238} -capture rate by activation of depleted uranium foils and subsequent γ -x-ray coincidence counting. The experimental results are compared with 26-group calculations using different methods and cross section sets.

Zusammenfassung

Zur Bestimmung von k_{∞} und Reaktionsratenverhältnissen wurde in der Nullenergieanlage SNEAK mit Anordnung 5 ein Experiment mit einem schnellen Reaktorgitter durchgeführt. Die Anordnung besteht aus einer zentralen Testzone, die radial und axial von Treiberzonen umgeben ist. Die innere Zone enthält Plättchen aus UO_2 - PuO_2 -Mischoxid, aus abgereichertem und natürlichem metallischen Uran, sowie Graphit als Moderator. Ihre Zusammensetzung wurde so gewählt, daß sich k_{∞} nahe 1 ergibt.

Die k_{∞} -Werte der Systeme mit verschiedenem C/ U^{238} -Verhältnis wurden durch die Messung der Reaktivitätsänderung beim Entleeren eines zentralen Bereichs der Testzone bestimmt. Die Spaltraten von U^{235} und U^{238} in der Zelle wurden mit Spaltspürzählern, die U^{238} -Einfangraten durch Aktivierung abgereicherter Uranfolien und anschließende γ -Zählung gemessen. Die Ergebnisse des Experiments werden mit 26-Gruppen-Rechnungen verglichen, bei denen verschiedene Methoden und Wirkungsquerschnittssätze angewendet wurden.

Introduction

Measurements of microscopic cross sections as well as a comparison of the critical mass of zero power fast assemblies with multigroup calculations have indicated that there are still rather large uncertainties in the nuclear data of the most important reactor materials, e.g. Pu²³⁹, Pu²⁴⁰, and U²³⁸, especially concerning the capture cross sections in the energy region from 100 eV to 15 keV (1,2).

Since a better knowledge of nuclear data in this energy range is needed for an accurate prediction of the breeding gain of large fast power reactors, the attention has turned to specially devised fast integral experiments which would give additional information on the low energy capture data and which serve as a check of nuclear data sets used in multigroup calculations.

A preferred method for such integral experiments is the so-called zero reactivity or PCTR-technique (3) known from investigations of thermal systems. It employs a two zone assembly whose central test zone is designed in such a way that its k_{∞} closely approaches unity. The exact value of k_{∞} can then be deduced from the reactivity change associated with the substitution of core material vs. void. In addition to k_{∞} the main reaction rates in the system can be studied by standard techniques.

Because of the zero leakage situation in the test zone a simple, i.e. non adjoint-weighted, neutron balance exists which allows to determine such reaction rates as capture in Pu²³⁹ that are difficult to measure directly in zero power systems.

In early 1969 experiments of this type were also performed at Karlsruhe on the zero power facility SNEAK, assembly 5. The main objective of the experimental program was to check present cross section sets and calculational methods on a fast system containing Pu²³⁹ and U²³⁸ as main fissile isotopes.

1. Description of SNEAK 5

1.1 Design Principles, Choice of the Test Lattice

The choice of the core configuration of SNEAK 5 was based on the following considerations:

- 1) In order to employ the PCTR-technique a two zone system is needed which is composed of a central test zone with $k_{\infty} \approx 1$ and a surrounding driver region to keep the entire system critical. The dimensions of the test zone should be chosen large enough, such that the neutron spectrum and the adjoint in its central region closely approach the equilibrium spectrum characteristic of an infinitely large system.
- 2) Axial and radial driver regions should be designed in such a way that flat flux distributions are established in both directions for the important energy groups.
- 3) As one wants to check the nuclear properties of systems containing Pu^{239} and U^{238} , it is desirable to keep the neutron production and absorption rate in the other materials as low as possible, e.g. by using a minimum quantity of structural stainless steel.
- 4) An additional moderating material is needed to soften the neutron spectrum and to enhance the influence of nuclear data in the low energy region (0.1 to 15 kev) on the measured integral parameters. Graphite was chosen as a moderator for easiness of the calculation.
- 5) Due to the soft neutron spectrum and the plate structure of the core materials rather large heterogeneity effects have to be accepted and appropriate corrections are necessary. In order to facilitate heterogeneity calculations as well as reaction rate measurements it is advantageous to choose a simple lattice structure for the test region.

The materials available for the test zone of SNEAK 5 are platelets (2 inch x 2 inch) which are stacked into the vertical stainless steel square tubes forming the matrix of the assembly. According to the previous considerations the following core materials were chosen for the test lattice

- 1) 20% PuO₂/UO₂ mixed oxide pellets canned in 0.28 mm stainless steel, plate thickness 1/4 inch,
- 2) natural uranium metal, 1/8 inch thick,
- 3) 0.4 % depleted uranium metal, 1/16 inch thick,
- 4) graphite, 1/8 inch thick.

A possible lattice structure with $k_{\infty} \approx 1$ was selected on the basis of zero dimensional homogeneous and heterogeneous calculations (cf. Sec.2) using the 26-group SNEAK-set (4). First calculations indicated that the cell structure SNEAK 5A (Fig.1), which consists of one natural uranium, one PuO₂/UO₂, one depleted uranium and seven graphite platelets, would give a k_{∞} -value slightly above 1 when the high Pu²³⁹ capture data (1) are used. This cell structure was chosen for the first assembly, SNEAK 5A.

Because of the uncertainty of nuclear data and calculation methods it was anticipated that the k_{∞} -value of SNEAK 5A might markedly deviate from 1 such that the composition of the test zone has to be modified in further steps. According to calculations (Table 4) k_{∞} can easily be adjusted by varying the amount of graphite contained in a cell.

In the experiments on SNEAK 5A its k_{∞} -value turned out 4% higher than originally expected (cf. Sec.3); this made it necessary to increase the number of graphite plates per cell to 10 and 13 in the following assemblies SNEAK 5B and 5C.

1.2 Description of the Assembly

The assemblies SNEAK 5A, 5B, and 5C, which differ mainly in the composition of the test zone, have a similar geometrical structure. As shown in Fig.2 and Fig.3 for SNEAK 5C, the assembly consists of a nearly cylindrical test zone (36 cm diameter, 76 cm height) surrounded by radial and axial driver regions, 15 cm and 20.5 cm thick, and a large 0.4 % depleted uranium metal blanket. The cell structure of the various regions is given in Fig.1. Due to the shortage of material a slight modification of the cell composition had to be made in the outer ring of the test zone (region 2) where depleted uranium platelets were replaced by natural uranium. A similar substitution was made in the driver (region 4) which is composed of uranium metal with an average enrichment of $\approx 20\%$ and additional moderating materials.

The 14 shim and safety rods of the fuel poison type are located in the driver region. In order to provide sufficient shutdown reactivity a higher fuel enrichment than in the normal core mixture was chosen. The driver region contained also two fuel elements with U^{235} - and U^{238} -fission chambers as monitors for the reaction rate measurements. Details of construction and operation of the SNEAK facility and its experimental equipment are given in a previous paper (5).

Table 1 shows some fundamental data of the SNEAK 5 assemblies. The atom densities for the homogenized zones, as derived from the standard cell patterns in Fig.1, are given in Table 2. Atom densities for the heterogeneous calculations in Table 3 were obtained by smearing the atom numbers of the individual platelets together with those of the corresponding steel of the matrix tube laterally over the area of one fuel element ($5.44 \times 5.44 \text{ cm}^2$). Finally, in Fig.3 an idealized reactor geometry for two-dimensional calculations has been derived by cylinderizing the zones of different loading patterns.

2. Multigroup Calculations

As a basis for the design of SNEAK 5 and for a discussion of experimental results a series of multigroup calculations were performed, using the Karlsruhe nuclear code system NUSYS. In these calculations the nuclear properties of the test zone as well as those of the entire assembly were studied.

2.1 Investigation of the Test Zone

Heterogeneous and zero-dimensional homogeneous calculations were performed to obtain information on k_{∞} of the test zone, the asymptotic real and adjoint spectra and the reaction rates for the individual nuclides. The 26-group SNEAK set (4), which uses the spectrum of a typical steam-cooled fast reactor as a weighting spectrum, served as a reference set. The following special problems were studied in these calculations:

- 1) The influence of the C/U-ratio on k_{∞} and the resulting neutron spectrum,
- 2) the effect of heterogeneity,
- 3) the influence of the weighting spectrum used in the cross section set on the elastic removal cross section, the resulting k_{∞} and the neutron spectrum.

The results of the homogeneous calculations in Table 4 show a marked decrease of k_{∞} with increasing C/U-ratio. This is explained by the softening of the spectrum and a decreasing resonance self-shielding which leads to an increase in U^{238} and Pu^{239} capture relative to the total fission source.

The heterogeneous calculations were performed with the ZERA code (6) for the cell structure shown in Fig.1, assuming infinite extension of the lattice in all directions. The ZERA code employs the collision probability method to solve the multigroup transport problem, considering space dependent resonance self-shielding.

Since the size of the SNEAK platelets is $5.07 \times 5.07 \text{ cm}^2$ whereas the lateral repetition length of the SNEAK matrix is 5.44 cm, two different atom densities were used as extremes. First, the material of the platelets was distributed uniformly in lateral directions to form slabs of the actual platelet thickness (I), second, slabs with the actual atom densities of the platelets were used (II). In both cases the stainless steel of the matrix tubes was uniformly distributed over the entire lattice. Thus, the first extreme underestimates the self-shielding, the second overestimates the self-shielding and the total fuel mass.

As a reference, a quasihomogeneous calculation with thin layers (1/1000 of the actual lattice dimensions) was run with the ZERA code. The result of this calculation differs slightly from the real homogeneous calculation, due to a somewhat different treatment of the self-shielding correction. Further calculations were done to determine the reactivity effect of the stainless steel matrix tubes and also the effect of a small concentration of Pu^{239} in the graphite, the latter as a basis for comparison with pile oscillator measurements on small Pu samples.

The results obtained with the SNEAK set (Table 4) show a rather large influence of heterogeneity on the multiplication constant k_{∞} . The difference $\Delta k^{het} = k^{het} - k^o$ is seen to increase from 3.4 %k for SNEAK 5A up to 6.8 %k for SNEAK 5C. The influence of heterogeneity on the spectrum is illustrated in Fig.5, where the spectra in the middle of the graphite region and in the middle of the PuO_2/UO_2 platelet are compared with the spectrum from the homogeneous calculation. Relative to the latter, the heterogeneous spectrum contains more neutrons in the high energy end, due to self-multiplication in the fuel, and

also at the low energy end due to a better moderation in the lumped graphite. With the shape of the adjoint, which has its minimum near 50 keV, a positive effect on k_{∞} results from this spectrum change.

Table 4 shows that the k_{∞} -change caused by adding graphite plates to the cell is greatly overestimated by the homogeneous calculation, since the latter overestimates the change in self-shielding of the U^{238} capture cross section. This is illustrated in Table 5 where the balance of reaction rates according to the various calculations is listed for assembly 5C.

Finally, homogeneous calculations were performed using for group 1 to 14 improved elastic removal cross sections which were found with the proper weighting spectrum of assembly 5. The spectrum from this improved calculation (Fig.4) also contains more neutrons at the high and low energy ends and leads to a positive change in k_{∞} of 1.6 %k.

2.2 Calculations for the Entire Assembly

Two-dimensional diffusion calculations were performed for assembly 5C using the idealized reactor geometry of Fig.3. In these calculations the following assumptions were made:

- 1) The reactor is of cylindrical geometry,
- 2) elements of the same composition are put together to form ring zones of the same area as the elements,
- 3) elements containing monitoring devices are substituted by regular elements of the same zone; those in the driver are corrected for, those in the blanket are not,
- 4) control rods are regarded as elements of the inner driver zone; the reactivity difference is calculated by considering them as a ring of their average composition; the poison part in the blanket is neglected.

The resulting k_{eff} and the power distribution for the various zones are given in Table 6. As a reference a homogeneous diffusion calculation (case 1) with the atom densities of Table 2 was done. In case 2 cell-averaged cross sections, as obtained from the heterogeneous ZERA-calculation, were used for the test zone. From the two-dimensional calculations also information on the flatness of neutron fluxes in the central region of the test zone was obtained. Table 7 gives the flux ratios $\phi_i(r = 6.9 \text{ cm})/\phi_i(o)$ and $\phi_i(z = 8.2 \text{ cm})/\phi_i(o)$ relative to the center. These ratios are seen to deviate from unity by less than $\pm 1.3 \%$ in the energy range from 10 eV to 10 MeV.

2.3. Spectrum Mismatch

The difference between the neutron spectrum at the center of the assembly and the equilibrium spectrum was studied in a series of homogeneous diffusion calculations using the SNEAK set:

- 1) The 26-group spectrum ϕ_i in the center of the actual assembly was found by two-dimensional or one-dimensional spherical calculations using a radius iteration for the driver zone to obtain $k_{\text{eff}} = 1$.
- 2) To derive the equilibrium spectrum ϕ_i^{as} a similar spherical calculation with $k_{\text{eff}} = 1$ was performed in which the dimension of the testzone was considerably enlarged ($R = 100$ cm) such as to establish a transient-free region in the center.
- 3) The static spectrum ϕ_i^{s} was obtained, as usual, from a zero-dimensional calculation with zero buckling and $k_{\text{eff}} = k_{\infty}$.

A comparison of the three spectra for assembly 5C is given in Fig.6 where the ratios $\phi_i/\phi_i^{\text{as}}$ and $\phi_i^{\text{s}}/\phi_i^{\text{as}}$ are plotted versus energy. The spectrum ϕ_i shows, relative to the equilibrium spectrum ϕ_i^{as} , a neutron deficiency at the high energy and low energy ends, leading to a spectrum mismatch of $\pm 2.5\%$ in the energy range above 10 eV. Also the static spectrum ϕ_i^{s} deviates from ϕ_i^{as} within $\pm 4\%$; it shows a hardening due to the increase of the fission source by the factor of $1/k_{\text{eff}}$ ($k_{\text{eff}} = 0.937$) in the static calculation.

For the evaluation of the experiments it may be important to know the influence of spectrum mismatch on k_{∞} . This effect was studied by calculating the "apparent" k_{∞} values defined by the ratio of neutron production to absorption in the different spectra,

$$k_{\infty}^* = \frac{\sum_{i=1}^G \nu \Sigma_{f_i} \phi_i}{\sum_{i=1}^G \Sigma_{a_i} \phi_i}, \quad k_{\infty}^{*\text{as}} = \frac{\sum_{i=1}^G \nu \Sigma_{f_i} \phi_i^{\text{as}}}{\sum_{i=1}^G \Sigma_{a_i} \phi_i^{\text{as}}}, \quad (3.1)$$

in addition to the static value

$$k_{\infty} = \frac{\sum_{i=1}^G \nu \Sigma_{f_i} \phi_i^{\text{s}}}{\sum_{i=1}^G \Sigma_{a_i} \phi_i^{\text{s}}}. \quad (3.2)$$

The symbols in eqs.(3.1) and (3.2) have the usual meaning of multigroup formalism ($G =$ number of groups).

The mismatch effect $k_{\infty}^* - k_{\infty}^{*\text{as}}$, as given in Tab. 4, is almost the same ($\approx -0.3\%$) for the three assemblies 5 A, 5 B and 5 C. But the deviation from the static value, $k_{\infty}^{*\text{as}} - k_{\infty}$, shows a rather strong variation as

illustrated in Fig. 7. According to calculations with different cross section sets for the three assemblies, $k_{\infty}^{* \text{ as}} - k_{\infty}$ may be considered as a linear function of k_{∞} which is nearly independent of the cross section set.

3. Cell Replacement Experiments

3.1 Zero Reactivity Method

The multiplication constant k_{∞} of the test lattices was determined by the zero reactivity (PCTR-) method which was originally developed to study the properties of thermal systems (3) and was later applied to fast assemblies (7). This method is based on the fact that in a region with zero leakage and unit k_{∞} no change in reactivity occurs when part of the core material is replaced by a void.

In an actual experiment, however, the condition $k_{\infty} = 1$ will not be met exactly and a finite reactivity change $-\Delta\rho$ will be observed when the sample of core material is taken out. In a region where the effect of neutron leakage is negligible, this reactivity change will be proportional to the net neutron production rate in the sample of volume V

$$\Delta\rho = K \cdot V \cdot \frac{\sum_{i=1}^G \nu \Sigma_{f_i} \phi_i - \sum_{i=1}^G \Sigma_{a_i} \phi_i}{\sum_{i=1}^G \Sigma_{a_i} \phi_i} = K \cdot V (k_{\infty}^* - 1), \quad (3.3)$$

where k_{∞}^* is defined by eq. (3.1).

For a given assembly the constant K has a distinct value which can, in principle, be obtained from multigroup calculations. Thus, eq.(3.3) gives a basis to determine the parameter k_{∞}^* from the measured reactivity worth $\Delta\rho$ of a lattice cell.

In our experiments a different procedure was used to evaluate k_{∞}^* . Instead of calculating K directly, the reactivity worth $\Delta\rho^{\text{Pu}}$ of a small Pu^{239} -sample in the center of the test zone was measured as a reference. Assuming the same amount of Pu^{239} to be distributed over each cell leads to a change in the multiplication constant

$$\Delta k_{\infty}^{*Pu} = k_{\infty}^{*Pu} - k_{\infty}^* = \Delta \rho^{Pu} / K \cdot V, \quad (3.4)$$

which can be calculated by heterogeneous methods with better confidence than K. Combination of eq.(3.3) and (3.4) yields the equation

$$\Delta \rho / \Delta \rho^{Pu} = (k_{\infty}^* - 1) / \Delta k_{\infty}^{*Pu}, \quad (3.5)$$

which allows to determine k_{∞}^* from $\Delta \rho / \Delta \rho^{Pu}$ and the calculated Δk_{∞}^{*Pu} . This calibration method has the advantage that measured reactivities enter as a ratio such that uncertainties of β_{eff} have no influence on the final result.

3.2 Experiments

The cell replacement experiments were performed in the center of the test zone of assembly 5A, 5B, and 5C within a region of about 15 cm diameter and 15 cm axial height. This region was considered small enough since the measured macroscopic traverses, Fig.13 and Fig.14, showed a variation <1% for the principal reaction rates.

The region to be voided comprised up to the 9 central elements and a total height of 5 cells (assembly 5A) or 3 cells (assembly 5B and 5C). Since the SNEAK fuel elements are suspended vertically and the steel walls of the matrix could not be entirely removed, the void experiment had to be performed in two steps:

- 1) Removal of the core platelets from the region to be voided and determination of the associated reactivity change per cell, $-\Delta \rho_c$,
- 2) insertion of additional tube material into the voided region and determination of the reactivity worth of the stainless steel contained in a cell, $\Delta \rho_s$.

Assuming additivity of both reactivity effects, $\Delta \rho = \Delta \rho_c + \Delta \rho_s$, eq.(3.3) is written

$$k_{\infty}^* - 1 = K \cdot V (\Delta \rho_c + \Delta \rho_s). \quad (3.6)$$

For the cell replacement experiments a set of special fuel elements was prepared as shown in Fig.8. In the central part of these elements the tube wall was cut out on one side such that the core material could easily be removed without unloading the remaining parts of the element. The platelets above the voided region were supported by small stainless steel frames which were fixed inside the tube at a position corresponding to the middle of the graphite region of the cell. Because of the simple cell structure it was possible to take out exact multiples of one cell in a region symmetrical to the midplane of the assembly.

The reactivity worths of the cell structure, $\Delta\rho_c$, and of additional tube material inserted into the voided region, $\Delta\rho_s$, were determined in a series of reactor runs at a preset power level of 8 Watts (corresponding to 0.9 ϵ sub-critical) by counterbalancing with a fine control rod which had been calibrated by the inverse kinetics method (8). Reproducibility studies indicated that the reactivity fluctuation is of the order of $\pm 0.06 \epsilon$ standard deviation per run, possibly due to mechanical positioning of the elements and temperature drifts.

For each assembly a series of experiments was devoted to the question whether the measured reactivity worth per cell depends on the size of the voided region. Experiments involving groups of one, four, and nine elements showed a clear trend of decreasing reactivity worth per cell with increasing void volume.

The reason for this effect is sought in the heterogeneous plate structure and its influence on the resonance self-shielding. When a single cell, for instance, is taken out from a complete regular lattice, the surface of the neighbouring uranium and plutonium platelets facing the voided region are exposed to "unshielded" slow neutrons coming from the graphite. This leads to an increase in U^{238} -capture in these surfaces (cf. the cell traverses in Fig.18) relative to the previous shielded situation and causes therefore an additional negative reactivity effect for the voided case. This tends to increase the measured cell worth. A similar effect is expected to arise from U^{238} -fission caused by uncollided fission neutrons coming from the neighbouring fuel platelets.

These considerations suggest that this heterogeneity effect is proportional to the uranium surface exposed to the void volume, while the ideal unperturbed reactivity worth is proportional to the volume of core material taken out. Thus, an extrapolation to zero surface was attempted in Fig.9 by plotting the measured reactivity worth $\Delta\rho_c'$ versus the number N_c of additional fuel package sides per cell of the voided region. A weighted least squares' fit yields straight lines for the three assemblies. Within experimental error no systematic trend in the slope of the lines with increasing C/U-ratio is seen. The extrapolated cell reactivity worths $\Delta\rho_c$ are listed in Table 8. The 5% relative error of these values is largely due to the uncertainty of the extrapolation.

The reactivity worth of stainless steel was determined by inserting additional tube material into the voided section. Measurements made in regions of different height and radial extension did not show any definite geometry dependence. This indicates that the diffusion terms arising from a flux curvature have a negligible influence on the measured reactivity worth. Within experimental error, the observed steel worth is proportional to the amount of steel added, showing that also self-shielding effects can be neglected.

3.3 Evaluation of k_{∞}^*

The total cell worth $\Delta\rho$ measured in assembly 5C was converted to k_{∞}^* by means of eq.(3.5). $\Delta\rho$ was normalized to the reactivity worth of an infinitely small Pu²³⁹-sample, $\Delta\rho^{\text{Pu}} = 460 \pm 10$ μ β per g, as found by extrapolation of the pile oscillator measurements in Fig.11(cf. Sec.4.1) to zero sample thickness. The corresponding k_{∞} -change was calculated in Table 4 by the ZERA code to be $\Delta k_{\infty}^{\text{Pu}} = 1.55 \times 10^{-2}$ per g Pu²³⁹ added to the graphite region of each cell. This leads to a k_{∞}^* -value of 1.030 ± 0.005 for assembly 5C, assuming a 10% accuracy of the normalization.

For assembly 5A and 5B no Pu²³⁹-sample measurements have been made. Here a normalization has been achieved on the basis of measured and calculated stainless steel worths. The results are shown in Table 8.

Finally, the measured k_{∞}^* was converted to the static k_{∞} by adding the calculated correction term $k_{\infty} - k_{\infty}^*$ given in Tab.4. This correction amounts to less than 0.3 %k.

4. Pile Oscillator Measurements

4.1 Reactivity Worth of Small Samples

The reactivity worth of small samples was measured in the central matrix position of SNEAK 5C by means of a vertical pile oscillator. The oscillator rod was a stainless steel square tube filled according to Fig.1 with platelets somewhat smaller ($4.66 \times 4.66 \text{ cm}^2$) than the regular ones such that the normal cell composition was only slightly perturbed. During the oscillation the central cell with the sample was periodically exchanged against a normal cell as a reference. The corresponding reactivity amplitude was derived from the signal of an ionization chamber by means of the inverse kinetics method and was corrected for linear drift (8).

Small-sample measurements have been made for U^{235} , U^{238} , Pu^{239} , and Pu^{240} , in some cases also as a function of sample size (cf. Table 9); the samples were placed at two cell positions: (1) in the center of the graphite region, (2) between the PuO_2/UO_2 and the natural uranium platelets. The experimental data were corrected for isotopes other than the principal ones.

In Fig.10 and Fig.11 the measured reactivity worths of U^{238} and Pu^{239} are shown as a function of sample thickness together with calculated values. These were obtained by a heterogeneous perturbation code based on collision probabilities (9), since a homogeneous treatment is inadequate because of the strong space dependence of the neutron spectrum and resonance self-shielding. The normal 26-group SNEAK set was used for these calculations, and the results were normalized to the measured worth of a small U^{235} sample in graphite.

The experimental data for U^{238} in graphite (Fig.10) show a much stronger sample size effect than calculated. This discrepancy indicates a softer spectrum in the graphite, possibly due to too high a capture cross section of U^{238} above 1 keV in the SNEAK set.

Additional calculations have been made for plutonium, using a modified SNEAK set (PuO2RE) which is based on the Gwin data for α - Pu^{239} (10) and the Pu^{240} cross sections of the Geel group (11). The results of these calculations are given in Table 10.

4.2 Determination of k_{∞}^*

Pile oscillator measurements were also used for a determination of k_{∞}^* by removing platelets from the central cell in several steps. The resulting reactivity changes are given in Table 11; they have been corrected for the somewhat smaller platelet size compared to the regular lattice.

The results may be interpreted as follows:

The optical thickness of the graphite is 1 1/2 mean free paths. Practically all neutrons that enter the fuel platelets will therefore have made at least one collision with the graphite. This means that the spectrum of the incoming neutrons will not have a resonance structure (narrow resonance approximation). Neutrons that have energies of the resonances of the fuel will be captured in the first few tenths of a mm. The capture rate of the fuel will thus decrease rapidly and then remain nearly constant (cf. Fig.18).

The reactivity effect of fuel that is added to an already existing fuel platelet is much less than if it were added in the graphite, see Fig.1. In the first case the reactivity effect is proportional to the capture rate after a few millimeters of fuel, that being the extra captures in the fuel. In the second case the reactivity effect is proportional to the capture rate in the sample. We therefore split the reactivity effect of the fuel into a volume proportional term and a term that is proportional to the surface of fuel to graphite.

We measure the volume proportional part, if we remove only part of the fuel, and measure the surface plus the volume proportional terms if we remove all the uranium in a layer. We measure the degradation effect of the graphite if we remove part of the graphite. Also we measure the degradation effect plus the surface effect of the fuel if we remove all the graphite in a layer, since the spectrum of the incoming neutrons in the uranium above and below the removed graphite layer will have a resonance structure.

The worth of a cell is then the degradation term of the graphite plus the volume proportional term of the fuel plus the surface effect of the fuel and the reactivity effect of the stainless steel element tubes.

The sum of the measurements 1 - 3 (Table 11) gives the volume proportional term of the fuel, since the surface of the fuel has not been altered. The difference of the measurement 5 and the sum of the measurements 1 - 3 gives twice the surface proportional term plus the effect of the extra surface of the sides of the surrounding platelets, since the fuel has two surfaces fuel to graphite. In the case that a cell is removed two such surfaces are removed. The degradation effect of graphite is determined by the removal of a thin layer of graphite.

The results may be summarized as follows:

Volume-proportional term of the fuel	3.65 m \$,
surface-proportional term of the fuel	- 1.05 m \$,
degradation of the graphite	- 0.70 m \$,
worth of the steel tube	<u>- 1.05 m \$,</u>
total worth of one cell	0.85 m \$.

This gives the following k_{∞}^* -values:

$$\begin{aligned}
 k_{\infty}^* &= 1.027 && \text{(normalization to U}^{235} \text{ in graphite),} \\
 k_{\infty}^* &= 1.030 && \text{(normalization to Pu}^{239} \text{ in graphite),} \\
 k_{\infty}^* &= 1.034 && \text{(normalization to Pu}^{239} \text{ in PuO}_2\text{/UO}_2\text{).}
 \end{aligned}$$

These results are consistent with those of the cell replacement experiments. The estimated error of k_{∞}^* is about 0.005.

5. Spectrum Measurement

The neutron spectrum from 20 to 1400 keV in the center of the test zone of assembly 5C has been measured by the proton recoil technique. One cylindrical counter (active length 7.4 cm, diameter 3.8 cm) filled with 3 atm methane and one spherical counter (3.94 cm diameter) filled with 2 atm hydrogen were used for these measurements. Gas type and high voltage were adjusted to cover the energy range of interest.

The proton recoil spectrum was corrected for wall effects and converted to the neutron spectrum as described in (12). Below about 60 keV the γ -n-discrimination technique (13) was employed.

Fig.12 gives a comparison of the measured neutron spectrum with homogeneous 26-group calculations, assuming zero geometrical buckling. Two calculated spectra are shown. The first was obtained with the original SNEAK set which is based on the weighting spectrum of a typical steam-cooled fast reactor; the second calculation was also found with the SNEAK set, but uses improved elastic removal cross sections which were obtained by weighting with the collision density spectrum of assembly 5C. The large difference in the elastic removal cross sections, especially in the energy range from 10 to 100 keV, leads to different shapes of the calculated spectra. As can be seen in Fig.12 the measured spectrum strongly supports the calculation with the improved removal data.

6. Measurement of Reaction Rates

For a more detailed comparison of the nuclear properties of fast test lattices with theoretical models it is important to determine the reaction rates in the system, especially those which contribute most to the overall neutron balance. As an illustration Table 5 gives the calculated contributions of the various reactions for assembly 5C. This table shows that 98% of the neutron production is due to fission in the main isotopes Pu^{239} , U^{235} , and U^{238} , while 66% of the neutron capture occurs in U^{238} and 22% in Pu^{239} .

In principle, the main fission rates as well as the capture rate in U^{238} can be measured accurately by standard techniques. On the other hand, no precision method exists so far to determine the Pu^{239} capture rate directly in zero power systems, since the α -active daughter product Pu^{240} has a long half life and is already present in substantial quantities in the normal plutonium fuel.

Indirect information on Pu^{239} capture can be obtained, however, by means of the neutron balance equation. For a zero leakage system it is written

$$k_{\infty}^* = \frac{\text{production rate}}{\text{absorption rate}} = \frac{\sum_x \bar{\nu}^x F^x}{\sum_x C^x + \sum_x F^x}, \quad (6.1)$$

where

$$F^x = \sum_i \phi_i \Sigma_{f_i}^x = \text{fission rate in nuclide } x \text{ per unit volume,}$$

$$C^x = \sum_i \phi_i \Sigma_{c_i}^x = \text{capture rate in nuclide } x \text{ per unit volume,}$$

$$\bar{\nu}^x = \frac{\sum_i \phi_i \nu \Sigma_{f_i}^x}{\sum_i \phi_i \Sigma_{f_i}^x} = \text{average number of fission neutrons for nuclide } x .$$

Solving for the average Pu²³⁹ capture to fission ratio, $\bar{\alpha}^{49} = C^{49}/F^{49}$, one finds

$$\bar{\alpha}^{49} = \frac{C^{49}}{F^{49}} = \sum_x \left(\frac{\bar{\nu}^x}{k_{\infty}^*} - 1 \right) \frac{F^x}{F^{49}} - \sum_{x \neq 49} \frac{C^x}{F^{49}}. \quad (6.2)$$

This equation allows to derive $\bar{\alpha}^{49}$ from ratios of the measurable fission and capture rates, F^{49} , F^{25} , F^{28} , C^{28} , the experimental k_{∞}^* -value, and calculated estimates for C^{25} and the other reaction rates of minor importance which occur in the stainless steel and the higher Pu-isotopes. Also the number of fission neutrons, $\bar{\nu}^x$, has to be taken from calculated spectra and principal nuclear data.

Eq.(6.2) gives $\bar{\alpha}^{49}$ as a difference of two numbers of comparable magnitude. The error analysis shows that for a 10% target accuracy of $\bar{\alpha}^{49}$ the measured ratio C^{28}/F^{49} has to be determined with a precision better than 2.5 %, while less stringent accuracy requirements exist for the other reaction rates. Although an absolute calibration of detectors with this accuracy can be achieved by present techniques, the problem remains to obtain experimental data that represent the average reaction rates inside the heterogeneous structure.

The original SNEAK 5 program was mainly oriented towards a determination of $\bar{\alpha}^{49}$ by means of eq.(6.2). However, due to difficulties in measuring the Pu²³⁹ fission rate inside the PuO₂/UO₂-platelet no $\bar{\alpha}^{49}$ -value could be obtained that is considered accurate enough for a meaningful comparison with nuclear data sets. Instead, the reaction rate studies in SNEAK 5 were concerned with three special problems:

- 1) Measurement of macroscopic radial and axial traverses to check the flatness of fluxes in the test region,
- 2) investigation of the spatial fine structure of reaction rates inside a lattice cell for a comparison with heterogeneous calculations,
- 3) determination of spatially integrated reaction rate ratios in the lattice for comparison with various multigroup calculations.

6.1 Macroscopic Fission and Capture Rate Traverses

Traverses of U^{235} - and U^{238} -fission rates and of the U^{238} -capture rate have been determined by foil irradiation as a check of the flux flatness in the test zone. The measurements were made along one radius and along the central axis of the assembly. Pairs of uranium metal foils of 0.1 mm thickness, 25 mm diameter, with different enrichment (0.2 and 20% U^{235}) were wrapped in to aluminium foil and placed inside the lattice in between the PuO_2/UO_2 and the natural uranium platelet.

The foils were counted on an automatic sample changer (14) using two NaJ-scintillation detectors. The induced fission product γ -activity above 660 keV was taken as a measure for the relative fission rate in the foil, and the contributions of U^{235} and U^{238} were derived from data of different foil enrichments. The U^{238} -capture rate has been determined by γ -x-ray coincidence counting at 106 keV (cf. Sec. 6.2.1).

Some results of these measurements are shown in Fig. 13 and Fig. 14, together with two-dimensional diffusion calculations for assembly 5C. The U^{235} -fission rate, n_f^{25} , shows a somewhat stronger curvature than the calculation which corresponds to a smaller k_{∞} . Plotted are also the ratios n_f^{28}/n_f^{25} and n_c^{28}/n_f^{25} ($n_{c,f}^x$ = fission or capture rate per atom of nuclide x) as spectral indices, each normalized to the calculation at the center. The variation of all these quantities is less than 1% within the region $r \leq 10$ cm, $z \leq 10$ cm, showing that only small spectrum changes occur in the energy region that contributes most to the neutron balance.

6.2 Fine Structure Measurements Inside the Lattice Cell

The fine structure of the U^{235} - and U^{238} -fission rates and of the U^{238} -capture rate was studied inside the central lattice cell of assembly 5C by irradiation of fission track detectors and uranium metal foils. For these measurements it was necessary to place the detector foil inside the fuel region perpendicular to the platelets in such a way that flux perturbations at the detector are kept low.

The experimental equipment used for the cell measurements is shown in Fig.15. It consists of a stainless steel box which contains part of the central cell, i.e. the package of fuel plates with the four neighbouring graphite platelets. The detector foil was embedded between two packages consisting of uranium metal platelets and UO_2/PuO_2 -platelets of about half the normal lateral dimensions ($2.4 \times 4.7 \text{ cm}^2$), which were clamped together by means of steel springs. The PuO_2/UO_2 -platelets contained oxide pellets machined to exact dimensions and enclosed in a 0.1 mm thick stainless steel can to secure easy handling of the materials. Streaming effects on the measured reaction rates due to the steel walls are considered negligible since the cell calculation shows relatively flat reaction rate distributions within the Pu-region (cf. Fig.16 and Fig.18).

6.2.1 Determination of U^{238} -Capture Rates

The U^{238} -capture rate per atom, n_c^{28} , was measured inside the fuel package by irradiation of 0.2 % depleted uranium metal foils and subsequent γ -x-ray counting.

To obtain average capture rates in each of the three fuel plates the cell arrangement of Fig. 15 was used. Three uranium foils, 0.06 mm thick and 10 mm long, were cut to the exact width of the corresponding fuel plates and placed between the two halves of the package. The halves were tightly pressed together to minimize streaming effects at the foil position.

A different experimental arrangement was chosen to determine the shape of the U^{238} -capture rate traverse inside the fuel. For these measurements uranium foils of 2.54 cm diameter, 0.08 mm thickness were placed parallel to the lattice structure between the various platelets of the central cell. Thus, the foil activity corresponds to the capture rate at distinct points of the lattice.

Several hours after the irradiation the γ -x-ray coincidence count rate was determined with two NaJ-scintillation detectors, using the automatic sample changer (14). The foil activities were corrected for natural background, foil weight and time in the usual manner. From the saturation activity $A_{\gamma\gamma}$ one obtains the capture rate

$$n_c^{28} = A_{\gamma\gamma} / \epsilon s_{\gamma\gamma} N^{28}, \quad (6.3)$$

where

ϵ = counting efficiency,
 N^{238} = number of U^{238} atoms per gram.

The γ -x-ray self-absorption in the foil was accounted for by a correction factor $s_{\gamma\gamma}$ given by the semiempirical formula

$$s_{\gamma\gamma} = \frac{1}{t} \int_0^t E_2(\mu x) E_2(\mu(t-x)) dx, \quad (6.4)$$

t = foil thickness,
 μ = 18.6 cm^{-1} .

This formula has been checked against direct self-absorption measurements and is known to represent the experimental data within about 1% (15). The overall counting efficiency ϵ needed for the absolute measurement has been determined by comparison with an Am^{243} -source calibrated within 1% by low-geometry α -counting (15).

6.2.2 Measurement of Fission Rates

The fine structure of the fission rates inside the fuel package has been investigated by the solid state track recorder (SSTR-) technique (16,17). This method is based on the fact that charged particles passing through an insulating material produce damage tracks which can be made visible under a microscope by applying a proper etching process. To measure fission rates by this method, a sample of fissile material is irradiated in close contact with the SSTR and the number of damage tracks produced by the fission fragments per unit area is counted. The main advantage of this method consists in the number of tracks being exactly proportional to the fission rate and the possibility to achieve a good spatial resolution.

For the fine structure measurements in SNEAK 5C the fissile sample with the SSTR was embedded between the two fuel packages of the central cell as shown in Fig.15. The sample was a deposit of $\approx 150 \mu\text{g}/\text{cm}^2 U_3O_8$ on a 0.1 mm thick stainless steel strip covered with a 0.04 mm thick foil of Makrofol N as a track recording material.

Fissile deposits of U^{235} and natural uranium were prepared by an electroplating process. The uranium layers were made highly adherent by adding to the electrolyte small amounts of $CeCl_3$. Irradiations inside the thermal column of STARK (18) showed that a good uniformity of the deposit has been achieved. It was also attempted to prepare samples of Pu^{239} using the same recipe. The deposits obtained so far, however, showed poor uniformity and could easily be wiped off. They could not be used for the cell measurements because of contamination problems and the impossibility of an accurate calibration.

After irradiation the SSTR-foils were etched in 6 n NaOH at $50^\circ C$ for about 40 min. Microphotographs were taken at different positions, each covering an area of about 1 mm^2 , and the number of tracks per unit area was counted visually with the help of a steel needle and an electromechanical register.

For the determination of U^{235} - and U^{238} -fission rates irradiations of a highly enriched U^{235} -sample and a U_{nat} -sample have been made, each at an individual power level to obtain a track density of about 3×10^3 per mm^2 convenient for visual evaluation. The measured track density was normalized to the count rate of a U^{238} -fission chamber as a monitor (cf. Fig.2). These normalized data of the two samples, Z_1 and Z_2 , were then converted to the fission rate n_f^x per atom of nuclide x, using the equations

$$\begin{aligned} Z_1 &= N_1^{25} n_f^{25} + N_1^{28} n_f^{28}, \\ Z_2 &= N_2^{25} n_f^{25} + N_2^{28} n_f^{28}, \end{aligned} \quad (6.5)$$

where

N_i^x = effective number of atoms of nuclide x per unit area of sample i.

As a basis for an absolute evaluation of n_f^{25} , n_f^{28} the amount of U^{235} of both samples, N_i^{25} , has been determined by calibration in a thermal flux, whereas the ratios N_i^{28}/N_i^{25} have been taken from the known foil enrichment. The calibration was done in the thermal column of the STARK reactor (18) against a highly enriched U^{235} -fission chamber of parallel plate type whose effective U^{235} -mass is known with an accuracy of 2%.

6.2.3 Comparison with Cell Calculations

Calculated and experimental reaction rate traverses for the central cell of SNEAK 5C are shown in Fig.16 to 18. They are normalized in such a way that the U^{235} fission rates n_f^{25} coincide for the center of the PuO_2/UO_2 platelet. The calculated curves have been obtained by the ZERA code using

- 1) the SNEAK set and laterally averaged atom densities for the platelets (case I in Table 4),
- 2) the SNEAK set and the actual atom densities for the platelets (case II in Tab. 4),
- 3) the MOXTOT set and laterally averaged atom densities.

The MOXTOT set is a modified SNEAK set described in (11) which includes the Gwin data (10) for Pu^{239} and the Moxon data (19) for U^{238} capture. This cross section change leads to a 12 % increase of Pu^{239} capture (Fig.17) and an 8 % decrease of U^{238} capture (Fig.18), but has only minor influence on the shape of the calculated traverses. Using the actual atom densities (case II) instead of the averaged ones results in a more pronounced fine structure, due to an increase in self-shielding.

The experimental fission rates found with the SSTR technique (Fig.16) appear to be consistent with the MOXTOT calculation, although a discrimination between the two cross section sets seems impossible regarding the given experimental uncertainties.

The U^{238} capture data found by foil activation are 8 % higher than the MOXTOT calculation and agree better with the SNEAK set. If the MOXTOT set is assumed to be more appropriate, one has to conclude that the spectrum contains more low-energy neutrons than calculated by the ZERA code.

Tab.12 gives a compilation of experimental and calculated reaction rate ratios in the PuO_2/UO_2 platelet and in the graphite region. The experimental data include Pu^{239}/U^{235} fission ratio measurements performed with calibrated miniature fission chambers (1.5 mm diameter) placed in the middle of the graphite region as well as between the two PuO_2/UO_2 half-platelets of Fig.15. In both cases the ratio n_f^{49}/n_f^{25} turned out to be substantially higher than the calculated values.

To determine the total fission and capture rates in the cell, F^{25} , F^{28} and C^{28} , the measured reaction rates per atom, n_f^{25} , n_f^{28} and n_c^{28} , were interpolated with the help of the ZERA calculation to render spatially averaged values $(\bar{n}_f^x)_j$, $(\bar{n}_c^x)_j$ for the three fuel plates (index j) of the package (cf. Tab.12). From these one finds the total reaction rates

$$F^x = \sum_{j=1}^3 (\bar{n}_f^x)_j N_j^x, \quad C^{28} = \sum_{j=1}^3 (\bar{n}_c^{28})_j N_j^{28}, \quad (6.6)$$

where

N_j^x ($j=1,2,3$) are the known total atom numbers of nuclide x in the three fuel plates of the regular lattice.

The resulting reaction rate ratios F^{28}/F^{25} and C^{28}/F^{25} are compared in Tab.13 with data obtained from the different multigroup calculations.

7. Discussion of Results

The measured k_{∞} of the SNEAK 5 assemblies is plotted in Fig.19 as a function of the C/U²³⁸ atom ratio. The experimental data are compared with homogeneous and heterogeneous 26-group calculations, using the original SNEAK set and also the modified SNEAK set MOXTOT, described in (11), which leads to k_{∞} -values 1.5 to 2 % higher than those given by the original SNEAK set.

In addition to the original homogeneous and heterogeneous calculations, corrected data are plotted which were obtained by adding to the heterogeneous k_{∞} a correction term Δk_{∞}^r to account for proper elastic removal cross sections in group 1 to 14 for the spectrum of SNEAK 5. This term has been taken from a homogeneous calculation, assuming additivity of heterogeneity and elastic removal effects on k_{∞} .

The experimental k_{∞} -data are seen to agree with the heterogeneous MOXTOT calculation corrected in the above manner. It should be born in mind, however, that the removal correction term may be in error by ≈ 1 % since no corrections have been made for neutron energies below group 14. Moreover, the question of additivity of both effects has to be checked by calculations using a larger number of energy groups.

The measured ratios of total reaction rates in the central cell of SNEAK 5C are compared in Tab.13 with different multigroup calculations. Relative to the heterogeneous MOXTOT calculation the measured uranium capture to fission ratio, C^{28}/F^{25} , is 9 % higher while the uranium fission ratio F^{28}/F^{25} is in satisfactory agreement. The miniature fission chamber measurement yields Pu^{239}/U^{235} fission ratios which deviate by +12 % in the graphite region and by +30 % inside the PuO_2/UO_2 platelet (cf.Tab.12). The latter measurement, however, seems to be affected by streaming inside the slot between the two separated half-platelets. The ratio F^{49}/F^{25} in Tab.13 has therefore been derived from the measurement in graphite, assuming the shape of the calculated fission rate traverses to be correct.

An evaluation of the Pu^{239} capture to fission ratio, α^{-49} , from k_{∞} and the measured data of Tab.13 on the basis of the neutron balance equation does not give a very significant check of the nuclear data, since the Pu^{239} fission rate measurement inside the PuO_2/UO_2 platelet could not be made with sufficient accuracy. If one uses the value $F^{49}/F^{25} = 11.8$ derived from the fission chamber measurement one finds, by means of eq.(6.2), a Pu^{239} capture to fission ratio $\alpha^{-49} = 0.57$ which is consistent with both the MOXTOT and the SNEAK calculation, since an experimental uncertainty of about ± 25 % has to be taken into account.

Acknowledgments

The authors gratefully acknowledge the continuous support by the operation staff of SNEAK during the experiments.

References

- (1) SCHOMBERG, M.G., M.G. SOWERBY, and F.W. EVANS: A New Method of Measuring Alpha (E) for Pu²³⁹. Fast Reactor Physics I, IAEA, Vienna, 1968, Proc. Symp. Karlsruhe, p.289-301 (1967).
- (2) KUESTERS, H. et al.: Analysis of Fast Critical Assemblies and Large Fast Power Reactors with Group-Constant Sets Recently Evaluated at Karlsruhe. KFK-793 (1968).
- (3) DONALUCE, D.J. et al.: Determination of k-Infinity from Critical Experiments with the PCTR. Nucl. Sci. Eng. 4, 297-321 (1958).
- (4) HUSCHKE, H.: Gruppenkonstanten für dampf- und natriumgekühlte schnelle Reaktoren in einer 26-Gruppendarstellung. KFK-770 (1968).
- (5) ENGELMANN, P. et al.: Construction and Experimental Equipment of the Karlsruhe Fast Critical Facility, SNEAK. Proc. Int. Conf. on Fast Critical Experiments and Their Analysis. Argonne, ANL-7320, 725-733 (1966).
- (6) WINTZER, D.: Heterogeneity Calculations Including Space Dependent Resonance Self-Shielding. KFK-633 (1967), and Fast Reactor Physics II, Vienna, p.237-255 (1968).
- (7) FOX, W.N. et al.: The Measurement of Pu²³⁹ Capture to Fission Ratios in Fast Reactor Lattices. J. Brit. Nucl. Energy Soc. 6, 63-79 (1967).
- (8) BORGWALDT, H. et al.: Experience Obtained at Karlsruhe with Different Kinetic Methods of Reactivity Determination. KFK-899 (1968).
- (9) OOSTERKAMP, W.J.: The Measurement and Calculation of the Reactivity of Samples in a Fast Heterogeneous Zero Power Reactor. KFK -1036
- (10) GWIN, R. et al.: WASH-1093, 106 (1968).
DE SAUSSURE, G.: Private communication from (11) (1968).
- (11) KIEFHABER, E. et al.: Evaluation of Fast Critical Experiments by Use of Recent Methods and Data. Fast Reactor Physics Conference (B.N.E.S.), London (1969).
- (12) BENJAMIN, P.W., D.D. KEMSHALL, and A. BRICKSTOCK: The Analysis of Recoil Proton Spectra. AWRE-Report O9/68 (1968).
- (13) BENNETT, E.F.: Fast Neutron Spectroscopy by Proton-Recoil Proportional Counting. Nucl. Sci. Eng. 27, 16-27 (1967).
- (14) BLANK, K.H. and H. SEUFERT: An Automatic Sample Changer with a Special Changing Method for γ - and $\gamma\gamma$ -Active Sources. Nucl. Instr. Meth. 46, 86-96 (1966).
- (15) SEUFERT, H. and D. STEGEMANN: A Method for Absolute Determination of U²³⁸ Capture Rates in Fast Zero-Power Reactors. Nucl. Sci. Eng. 28, 277-285 (1967).
- (16) FLEISCHER, R.L., P.B. PRICE, and R.M. WALKER: Solid State Track Detectors: Applications to Nuclear Science and Geophysics. Ann. Rev. Nucl. Sci. 15, 1 (1965).
- (17) GOLD, R., R.J. ARMANI, and J.H. ROBERTS: Absolute Fission Rate Measurements with Solid-State Track Recorders. Nucl. Sci. Eng. 34, 13 (1968).
- (18) BARLEON, L. et al.: Evaluation of Reactor Physics Experiments on the Coupled Fast-Thermal Argonaut Reactor STARK. Proc. Int. Conf. on Fast Critical Experiments and Their Analysis, Argonne, ANL-7320, 137-158 (1966).
- (19) MOXON, M.C. et al.: To be published.
MOXON, M.C. and E.R. RAE: Private communication from (11) (1969).

Assembly	5A	5B	5C	
<u>Test zone:</u>				
Volume	303.6	292.7	278.9	l
Mass Pu ²³⁹	90.1	78.9	48.6	kg
Atom ratio C/U ²³⁸	6.523	9.317	12.113	
Atom ratio C/Pu ²³⁹	69.18	98.82	128.46	
<u>Driver zone:</u>				
Volume	446.9	459.6	463.4	l
Mass U ²³⁵	564.7	580.7	585.4	kg
Average enrichment	18.7	18.7	18.7	% U ²³⁵
<u>Calculated power split⁽¹⁾:</u>				
Test zone	22.9	-	15.4	%
Driver	70.7	-	76.2	%
Blanket	7.0	-	8.4	%
Calculated k_{eff} ⁽²⁾	$6.071 \cdot 10^{-3}$	$6.207 \cdot 10^{-3}$	$6.294 \cdot 10^{-3}$	

(1): From 2-dimensional calculation

(2): From 1-dimensional spherical calculation

Table 1: Fundamental Data of the SNEAK 5 Assemblies

Region/Assembly	Al	C	Co	Cr	Fe	H	Mg	Mn	Mo	Nb
1 test zone, 5A	2,2826'-6	5.1779'-2		1.4294'-3	5.0927'-3		1.0133'-6	9.4052'-5	1.1833'-5	8.6361'-6
test zone, 5B	1,7755'-6	5.7532'-2		1.358' -3	4.8399'-3		7.8823'-7	9.2581'-5	1.1419'-5	8.6157'-6
test zone, 5C	1.4533'-6	6.1217'-2		1.3127'-3	4.6793'-3		6.4519'-7	9.1646'-5	1.1156'-5	8.6026'-6
2 test zone, 5A+B	2.2826'-6	5.1778'-2		1.4294'-3	5.0927'-3		1.0133'-6	9.4052'-5	1.1833'-5	8.6361'-6
test zone, 5C	1.0812'-6	6.5393'-2		1.2603'-3	5.0927'-3		4.8' -7	9.0567'-5	1.0852'-5	8.5876'-6
3 driver	5.49896'-3	2.2698'-2	1.1593'-5	2.4599'-3	8.6919'-3	1.05316'-3	2.0927'-5	1.3936'-4	2.1807'-5	8.544' -6
4 driver	1.99346'-2	5.5244'-4	1.1593'-5	2.4599'-3	8.6919'-3	1.05316'-3	1.6877'-4	1.917' -4	2.1807'-5	8.544' -6
5 blanket		1.356' -5		1.1081'-3	3.9549'-3			8.743' -5	9.97' -6	8.544' -6

Region/Assembly	Ni	O	Pu ²³⁹	Pu ²⁴⁰	Pu ²⁴¹	Pu ²⁴²	Si	Ti	U ²³⁵	U ²³⁸
1 test zone, 5A	8.5509'-4	6.1999'-3	7.48475'-4	6.72383'-5	6.1107'-6	3.0707'-7	5.8934'-5		5.19378'-5	7.93822'-3
test zone, 5B	7.9227 -4	4.8226'-3	5.82206'-4	5.23017'-5	4.7532'-6	2.3886'-7	5.5909'-5		4.04001'-5	6.17487'-3
test zone, 5C	7.5235'-4	3.9475'-3	4.76555'-4	4.28107'-5	3.8907'-6	1.9551'-7	5.3988'-5		3.30689'-5	5.05435'-3
2 test zone, 5A+B	8.3986'-4	6.1999'-3	7.48475'-4	6.72383'-5	6.1107'-6	3.0707'-7	5.8934'-5		5.82591'-5	7.99523'-3
test zone, 5C	6.9904'-4	2.9368'-3	3.5454' -4	3.18497'-5	2.8945'-6	1.4545'-7	5.1768'-5		2.75964'-5	3.78721'-3
3 driver	1.5069'-3	8.2694'-3					1.1172'-4	2.4479'-5	3.23712'-3	1.40784'-2
4 driver	1.5069'-3	8.2694'-3					2.3258'-4	2.4479'-5	3.23712'-3	1.40784'-2
5 blanket							4.532' -5		1.6245' -4	3.994' -2

Table 2: Homogenized Atom Densities ($10^{24}/\text{cm}^3$) in SNEAK 5

Platelet	Al	C	Cr	Fe	Mo	Ni	O	Pu ²⁴⁰	Pu ²⁴¹	Pu ²³⁹	Si	U ²³⁵	U ²³⁸
Graphite	0	7.7747'-2	1.1081'-3	3.9549'-3	9.97' -6	5.7230'-4					4.532' -5		
PuO ₂ /UO ₂	1.2'-5	6.2417'-5	2.7972'-3	9.9361'-3	1.9763'-5	1.4572'-3	3.2592'-2	3.5346'-4	3.2123'-5	3.9346'-3	1.1688'-4	8.7437'-5	1.1876'-2
U _{depl.}	0	1.3560'-5	1.1081'-3	3.9549'-3	9.97' -6	1.588' -3					4.532' -5	1.5884'-4	3.9009'-2
U _{nat.}	0	1.3560'-5	1.1081'-3	3.9549'-3	9.9700'-6	1.2678'-3					4.532' -5	2.9176'-4	4.0205'-2

These densities are based on 0.314 mm thickness of the platelets. They were used only in heterogeneity calculations and are not totally consistent with those in Table 2. The steel of the fuel element tubes is smeared out over the whole platelet, the area of the platelet is assumed to be that of the squared fundamental repetition length of the core matrix (= 5.44 cm).

Table 3: Atom Densities ($10^{24}/\text{cm}^3$) in the Platelets for Heterogeneity Calculations

Assembly	5A	5B	5C	5C +)
C/U ²³⁸ -ratio	6.52	9.32	12.11	12.11
Homogeneous calculation k_{∞} Worth of steel matrix Δk_{∞}^s	0.9935 $-3.446 \cdot 10^{-2}$	0.9628 $-3.789 \cdot 10^{-2}$	0.9370 $-4.039 \cdot 10^{-2}$	0.9530
Heterogeneous calculation (I) k_{∞}^{het} $\Delta k_{\infty}^{het} = k_{\infty}^{het} - k_{\infty}^o$ Heterogeneous calculation (II) k_{∞}^{het} $\Delta k_{\infty}^{het} = k_{\infty}^{het} - k_{\infty}^o$ Quasihom. calcul. (I) k_{∞}^o	1.0242 $3.37 \cdot 10^{-2}$ 1.0318 $4.13 \cdot 10^{-2}$ 0.9905	1.0115 $5.11 \cdot 10^{-2}$ 1.0206 $6.02 \cdot 10^{-2}$ 0.9604	1.0027 $6.78 \cdot 10^{-2}$ 1.0121 $7.72 \cdot 10^{-2}$ 0.9349	1.0177
Heterogeneous calculation (I) Worth of steel matrix (Δk_{∞}^s) ^{het} Δk_{∞} of 10^{19} at/cm ³ Pu ²³⁹ in graphite region Δk_{∞} per 1g Pu ²³⁹ /cell	-	-	$-4.26 \cdot 10^{-2}$ $0.744 \cdot 10^{-2}$ $1.55 \cdot 10^{-2}$	
Homogeneous calcul. with removal correct. k_{∞}^r Effect of removal correction $\Delta k_{\infty} = k_{\infty}^r - k_{\infty}^o$	1.0119 $1.83 \cdot 10^{-2}$	0.9809 $1.81 \cdot 10^{-2}$	0.9529 $1.59 \cdot 10^{-2}$	0.9664 $1.34 \cdot 10^{-2}$
$k_{\infty}^* - k_{\infty}^{*as}$ $k_{\infty}^{*as} - k_{\infty}^o$	$-0.273 \cdot 10^{-2}$ $-0.088 \cdot 10^{-2}$	$-0.283 \cdot 10^{-2}$ $-0.341 \cdot 10^{-2}$	$-0.285 \cdot 10^{-2}$ $-0.463 \cdot 10^{-2}$	
+) Using modified SNEAK set (MOXTOT (11)).				

Table 4: Homogeneous and Heterogeneous k_{∞} -Calculations with SNEAK set

	Production, $\sum_i \phi_i \nu \Sigma_{f_i}$				Fission, $\sum_i \phi_i \Sigma_{f_i}$				Capture, $\sum_i \phi_i \Sigma_{c_i}$				
	A	B	C	D	A	B	C	D	A	B	C	D	
U ²³⁵	6.04	5.99	-	6.09	2.47	2.45	2.66	2.50	1.23	1.24	1.40	1.25	
U ²³⁸	10.08	9.87	-	9.70	3.59	3.50	3.62	3.46	50.03	48.15	42.90	46.54	
Pu ²³⁹	81.96	82.20	-	82.32	28.10	28.17	27.84	28.24	15.13	15.38	14.20	17.19	
Pu ²⁴⁰	0.57	0.61	-	0.71	0.19	0.20	0.20	0.22	2.44	2.48	2.82	1.96	
Pu ²⁴¹	1.35	1.33	-	1.18	0.46	0.45	0.49	0.40	0.10	0.10	0.11	0.14	
Steel	-	-	-	-	-	-	-	-	3.02	2.86	3.26	3.05	
C + O	-	-	-	-	-	-	-	-	0.09	0.10	0.10	0.09	
Total	100	100	100	100	34.81	34.77	34.81	34.82	72.04	70.31	64.79	70.22	
									α^{-49}	0.539	0.546	0.510	0.608

A : Homogeneous, SNEAK set.

B : Homogeneous, SNEAK set with improved elastic removal data.

C : Heterogeneous, SNEAK set.

D : Homogeneous, modified SNEAK set (MOXTOT).

Table 5: Calculated Balance of Reaction Rates in Assembly 5C

	Power split			k_{eff} for idealized system	k_{eff} for real system with control rods
	Test zone	Driver	Blanket		
(1) Hom. calculation with SNEAK set	15.4 %	76.2 %	8.4 %	0.9611	
(2) Hom. calculation, using cell-averaged cross sections from ZERA	18.9 %	73.3 %	7.8 %	0.9790	
Experiment	-	-	-		1.0049

Table 6: Results of Two-Dimensional Calculations for SNEAK 5C

Group-No. i	Energy	$\phi_i(r=6.9 \text{ cm})/\phi_i(o)$	$\phi_i(z=8.2 \text{ cm})/\phi_i(o)$
1	6.5-10.5 MeV	0.9991	1.0047
2	4.0-6.5 MeV	0.9980	1.0030
3	2.5-4.0 MeV	0.9973	1.0019
4	1.4-2.5 MeV	0.9976	1.0024
5	0.8-1.4 MeV	0.9980	1.0031
6	0.4-0.8 MeV	0.9990	1.0049
7	0.2-0.4 MeV	1.0002	1.0070
8	0.1-0.2 MeV	1.0016	1.0093
9	46.5-100 keV	1.0029	1.0113
10	21.5-46.5 keV	1.0038	1.0126
11	10.0-21.5 keV	1.0040	1.0127
12	4.65-10.0 keV	1.0036	1.0119
13	2.15-4.65 keV	1.0024	1.0098
14	1.0-2.15 keV	1.0007	1.0068
15	465-1000 eV	0.9985	1.0032
16	215-465 eV	0.9962	0.9995
17	100-215 eV	0.9938	0.9958
18	46.5-100 eV	0.9920	0.9930
19	21.5-46.5 eV	0.9900	0.9898
20	10.0-21.5 eV	0.9888	0.9877
21	4.65-10 eV	0.9875	0.9856
22	2.15-4.65 eV	0.9848	0.9809
23	1.0-2.15 eV	0.9839	0.9792
24	0.465-1.0 eV	0.9829	0.9775
25	0.215-0.465 eV	0.9828	0.9774
26	0.0252	0.9827	0.9771

Table 7: Flux Ratios in the Center of SNEAK 5C.
Two-dimensional calculation with SNEAK set.

Assembly	5A	5B	5C	
C/U-ratio	6.52	9.32	12.11	
Extrapolated worth of core material per cell $\Delta\rho_c$	2.18 \pm 0.10	2.05 \pm 0.10	1.90 \pm 0.10	m g/cell
Worth of stainless steel per gram	-1.22 \pm 0.09	-1.22 \pm 0.09	-1.225 \pm 0.09	10 ⁻² m g/g
Worth of fuel tube material per cell $\Delta\rho_s$	-0.63 \pm 0.05	-0.81 \pm 0.06	-1.00 \pm 0.08	m g/cell
Total cell worth $\Delta\rho = \Delta\rho_c + \Delta\rho_s$	1.55 \pm 0.12	1.24 \pm 0.12	0.90 \pm 0.13	m g/cell
Reactivity ratio - $\Delta\rho_c / \Delta\rho_s$	3.45 \pm 0.35	2.52 \pm 0.25	1.90 \pm 0.20	
Measured Pu ²³⁹ worth per g Pu $\Delta\rho$	-	-	0.460 \pm 0.010	m g/g
Calculated Δk_{∞}^{Pu} for 1 g Pu ²³⁹ per cell	-	-	1.55 · 10 ⁻²	$\Delta k/g$
Resulting k_{∞}^*	1.069 \pm 0.009	1.047 \pm 0.007	1.030 \pm 0.005	
$k_{\infty}^* - k_{\infty}$	0.003	0.000	-0.001	
Resulting k_{∞} of the test lattice	1.066 \pm 0.009	1.047 \pm 0.007	1.031 \pm 0.005	

Table 8: Results of the Cell Replacement Experiments

Thickness of Pu ²³⁹ (g/cm ²):	0.1	0.15	0.3	0.6	Pu ²⁴⁰	Fe ₂ O ₃
Pu ²³⁹ (g) :	1.22	2.04	4.06	8.12	0.02	-
Pu ²⁴⁰ (g) :	0.11	0.18	0.35	0.70	2.70	-
Pu ²⁴¹ (g) :	-	-	-	-	0.02	-
Fe (g) :	3.0	2.0	2.0	4.0	1.9	21
O (g) :	0.2	0.3	0.6	1.2	0.4	0.9

Table 9: Composition of the Plutonium Samples

Sample:	Reactivity worth (ρ β /g)		
	SNEAK-set ¹⁾	PuO2RE-set ¹⁾	Experiment
60 g U ²³⁸ in C	- 43.8	- 42.8	- 37.7 \pm 0.2
60 g U ²³⁸ in U _{nat}	- 30.8	-	- 24.4 \pm 0.2
5 g U ²³⁸ in C	- 67	- 67	- 86 \pm 3
5 g Pu ²³⁹ in C	486	460	443 \pm 5
5 g Pu ²³⁹ in U _{nat}	464	437	390 \pm 5
3 g Pu ²⁴⁰ in C	-244	-165	-170 \pm 5
3 g Pu ²⁴⁰ in U _{nat}	-180	-113	-104 \pm 5
1 g U ²³⁵ in C	435	435	435 \pm 3

1) Normalized to experiment for 1 g U²³⁵ in C.

Table 10: Central Reactivity Worth Calculation for SNEAK 5C with Heterogeneous Perturbation Code

	Sample	Measured reactivity worth
1	Depleted uranium , 1.6 mm	- 2.02 m β
2	Natural uranium , 3.1 mm	- 3.96 m β
3	PuO ₂ /UO ₂ , 6.2 mm	+ 9.61 m β
4	Graphite , 3.1 mm	+ 0.055 m β
5	Depleted uranium , 1.6 mm + PuO ₂ /UO ₂ , 6.2 mm + natural uranium, 3.1 mm	+ 2.15 m β
6	Entire Cell: depleted uranium , 1.6 mm + PuO ₂ /UO ₂ , 6.2 mm + natural uranium, 3.1 mm + graphite , 40.8 mm	+ 2.15 m β

Table 11: Reactivity Worth of Platelets vs. Void in the Central Cell of SNEAK 5C

Tab. 12: Fission Ratios in the Central Cell of SNEAK 5 C.

	Experiment	SNEAK set		MOXTOT set
		Heterogeneous (I)	Heterogeneous (II)	Heterogeneous (I)
Middle of Pu-platelet:				
n_f^{28} / n_f^{25}	0.0099+0.0005	0,01029	0,01055	0.00982
n_c^{28} / n_f^{25}	0.104 +0.004	0,1061	0.1047	0.0974
n_f^{49} / n_f^{25}	-	0.7325	0.7271	0.7292
Average over Pu-platelet				
n_f^{-28} / n_f^{-25}	0.0094+0.0005	0.00997	0.01018	0.00952
n_c^{-28} / n_f^{-25}	0.106 +0.004	0.1050	0.1034	0.0965
n_f^{-49} / n_f^{-25}	1.00 +0.05 ⁽¹⁾	0.7564	0.7537	0.7529
Middle of Graphite				
n_f^{28} / n_f^{25}	=			0.00637
n_c^{28} / n_f^{25}	-			0.5841
n_f^{49} / n_f^{25}	1.055+0.03 ⁽²⁾			0.9369

(1) Miniature fission chamber in slot between 2 PuO₂/UO₂ half-platelets

(2) Fission chamber in graphite region

	Experiment	SNEAK set				Mod. SNEAK set (MOXTOT)	
		Homogeneous	Hom., with removal corr.	Heterogen. (I)	Heterogen. (II)	Homogeneous	Heterogen. (I)
Total ratios:							
F^{28}/F^{25}	1.29+0.06	1.452	1.424	1.365	1.366	1.390	1.302
F^{49}/F^{25}	11.80 (1)	11.36	11.49	10.50	10.35	11.32	10.43
C^{28}/F^{25}	16.3 ± 0.5	20.20	19.63	16.15	16.31	18.70	14.90
$\frac{49}{\alpha}$	0.57 (2)	0.539	0.546	0.510	0.505	0.608	0.574

(1): From fission chamber measurement

(2): Derived from neutron balance, eq.(6.2)

Table 13: Reaction Rate Ratios in the Central Cell of SNEAK 5C

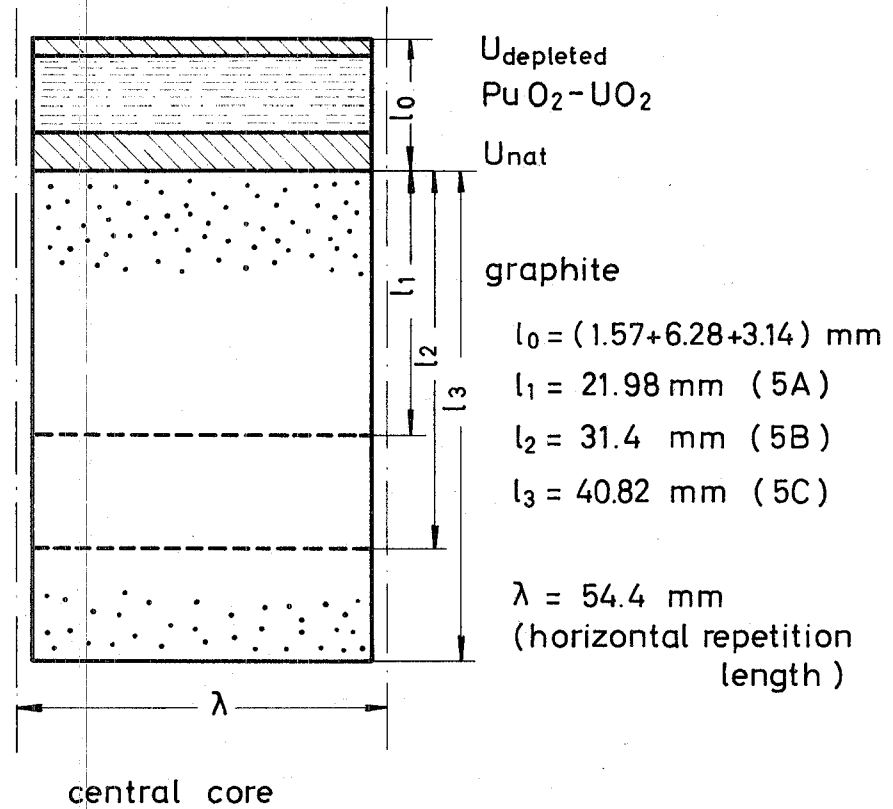
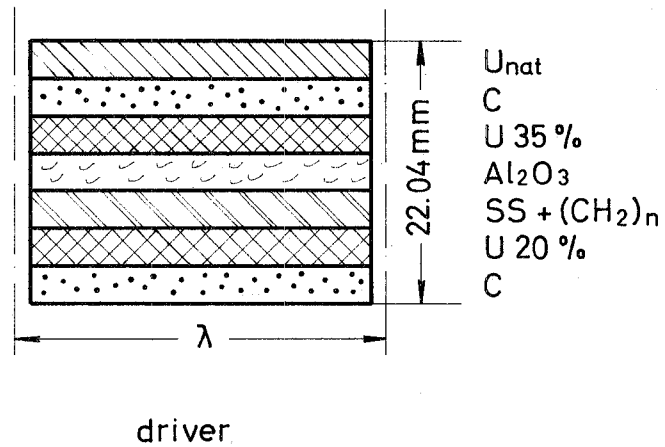


Fig. 1: Principal Cell Structures of SNEAK 5

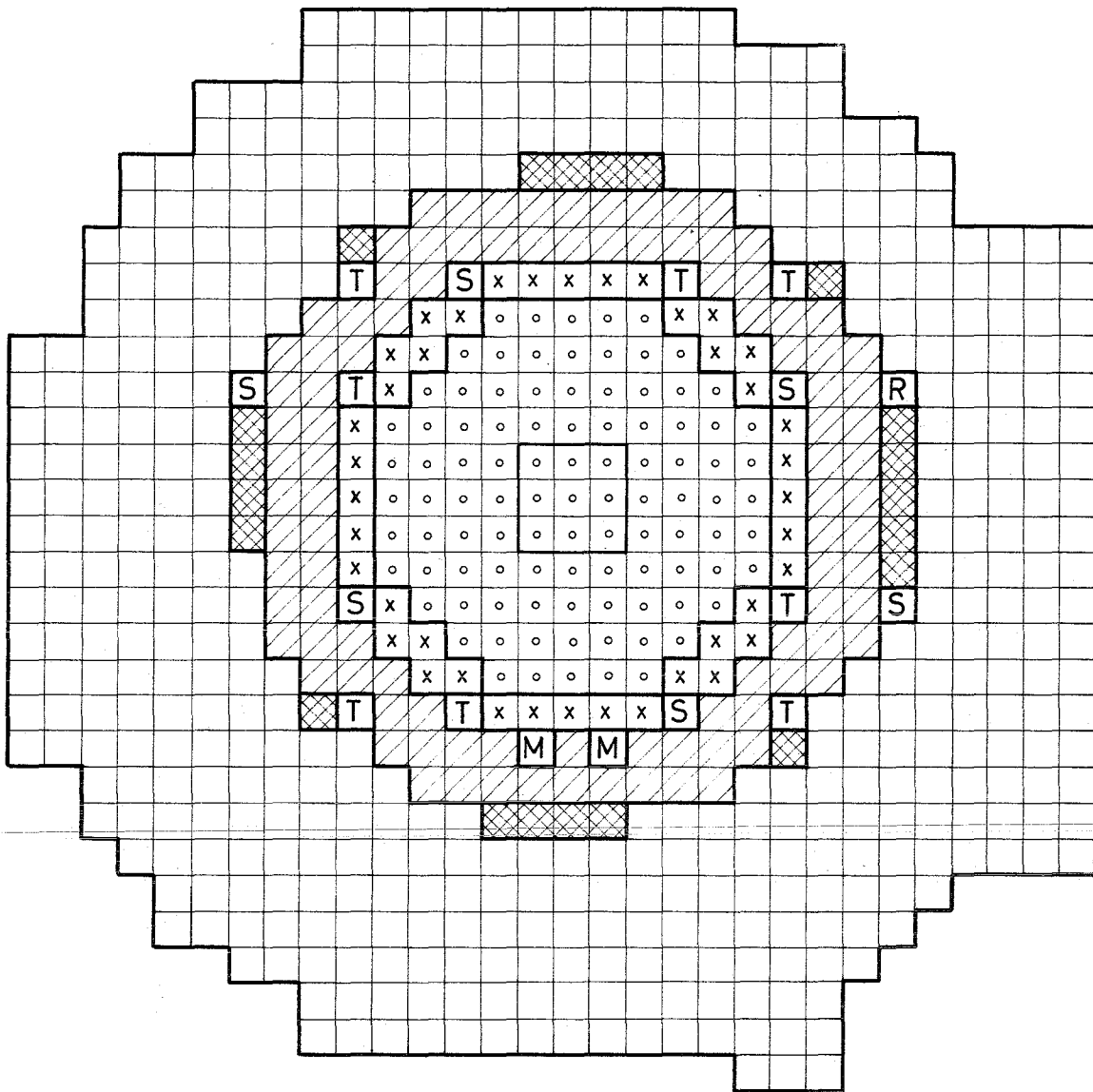
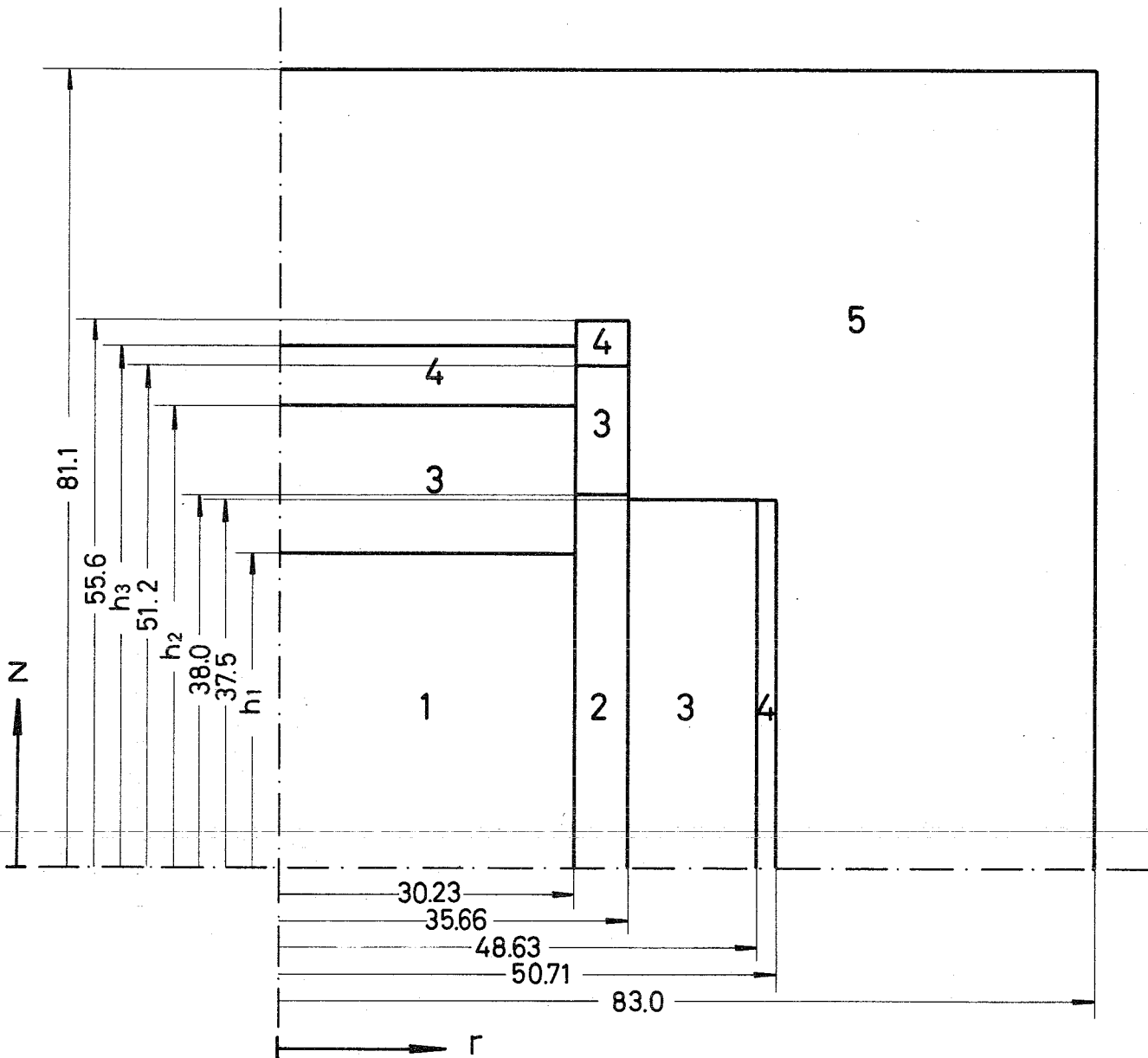


Fig.2 : Cross Section of SNEAK 5C

- | | | | |
|---|----------------------|---|----------------------|
| ○ | test zone , region 1 | × | test zone , region 2 |
| ▨ | driver , region 3 | ⊠ | driver , region 4 |
| □ | blanket | | |
| S | safety rod | | |
| T | shim rod | | |
| R | fine control rod | | |
| M | monitor | | |

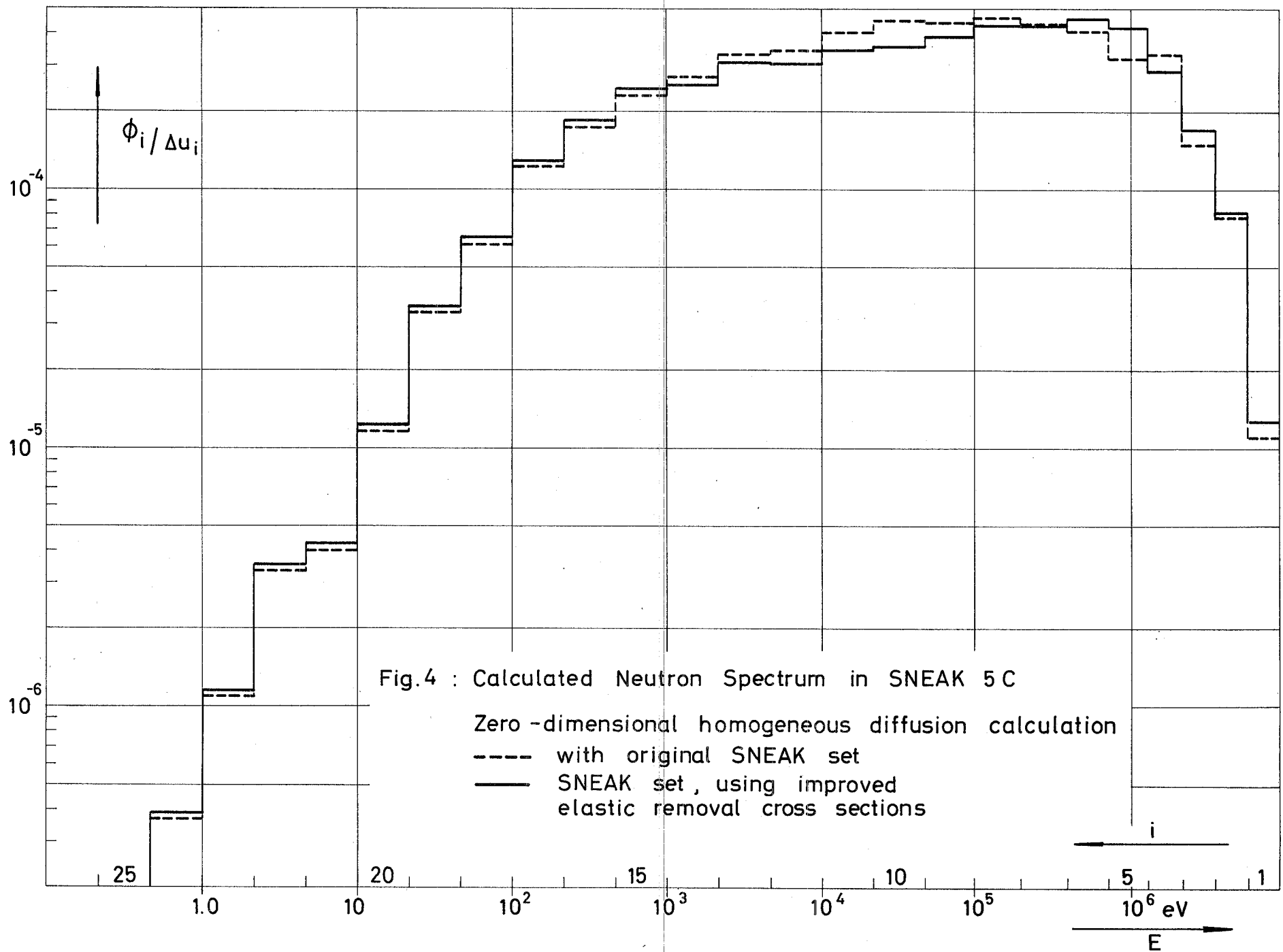


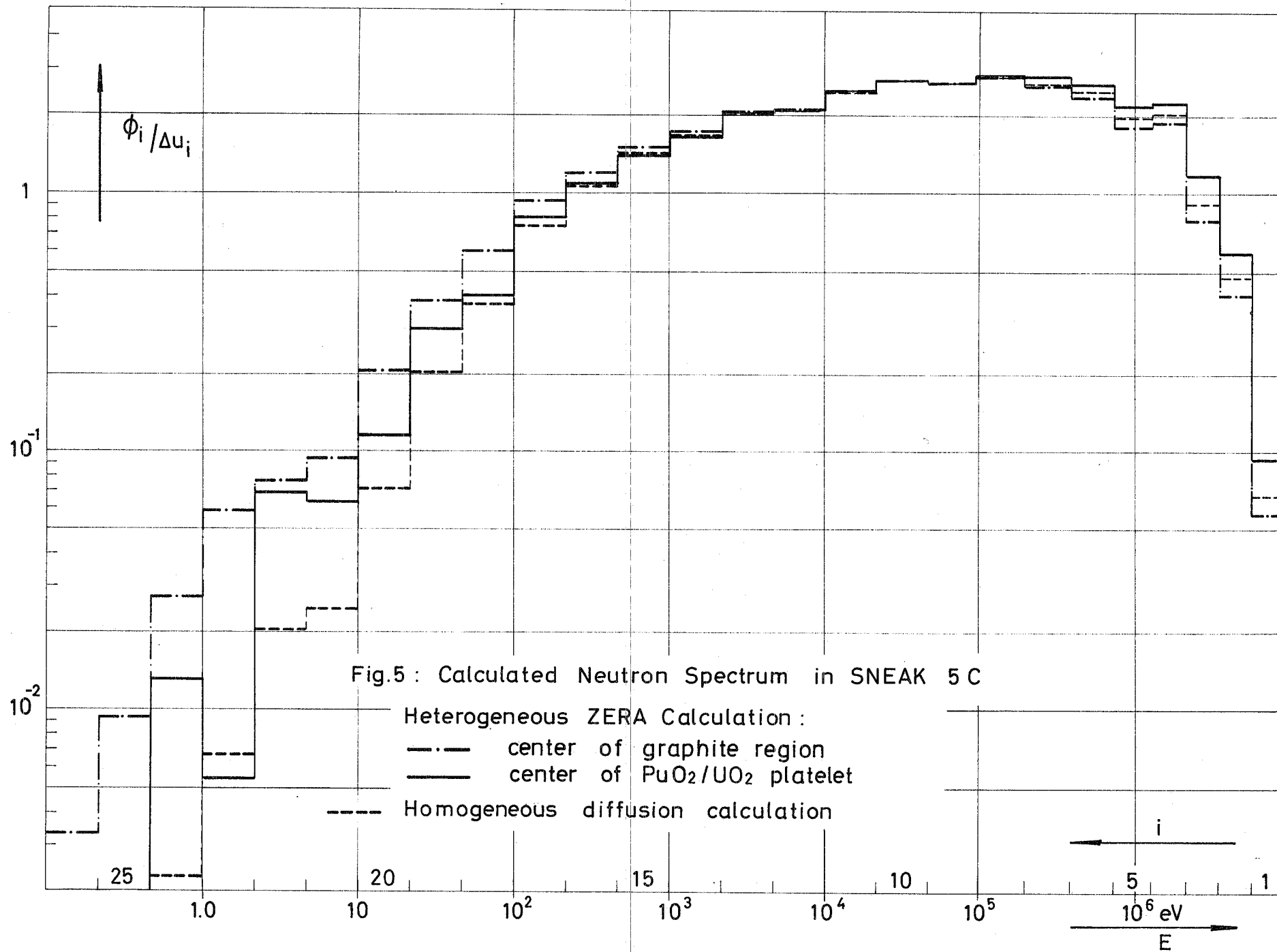
	5 A	5 B	5 C
h_1	38.0	36.1	33.7
h_2	51.2	49.3	46.9
h_3	55.6	55.9	54.2

Fig. 3: Idealized Reactor Geometry of SNEAK 5

region 1 }
 region 2 } test zone
 region 3 }
 region 4 } driver zone
 region 5 } blanket

(dimensions in cm)





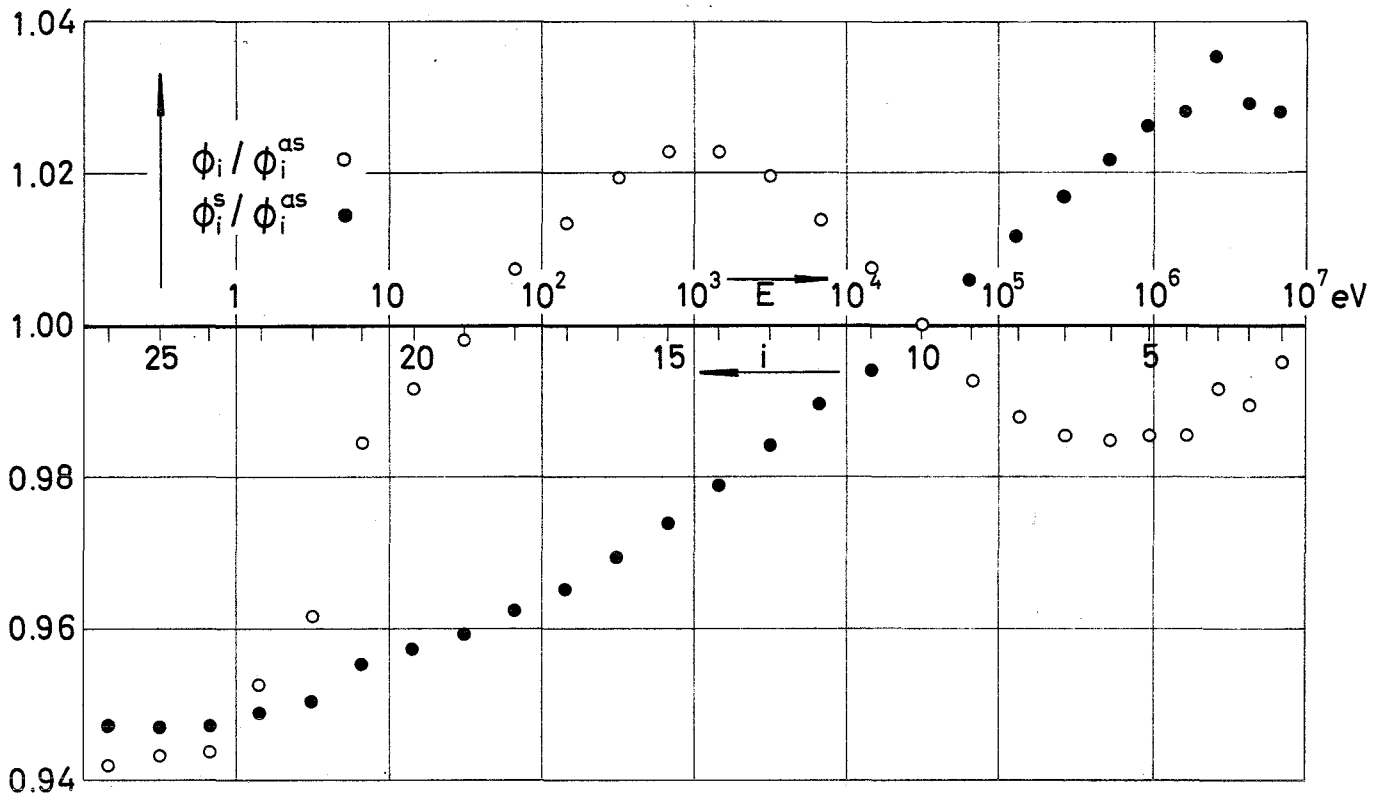


Fig.6 Deviation of the Neutron Spectra ϕ_i and ϕ_i^s from the Equilibrium Spectrum ϕ_i^{as} for SNEAK 5C.
(Homogeneous calculations with SNEAK set normalized for $i=10$)

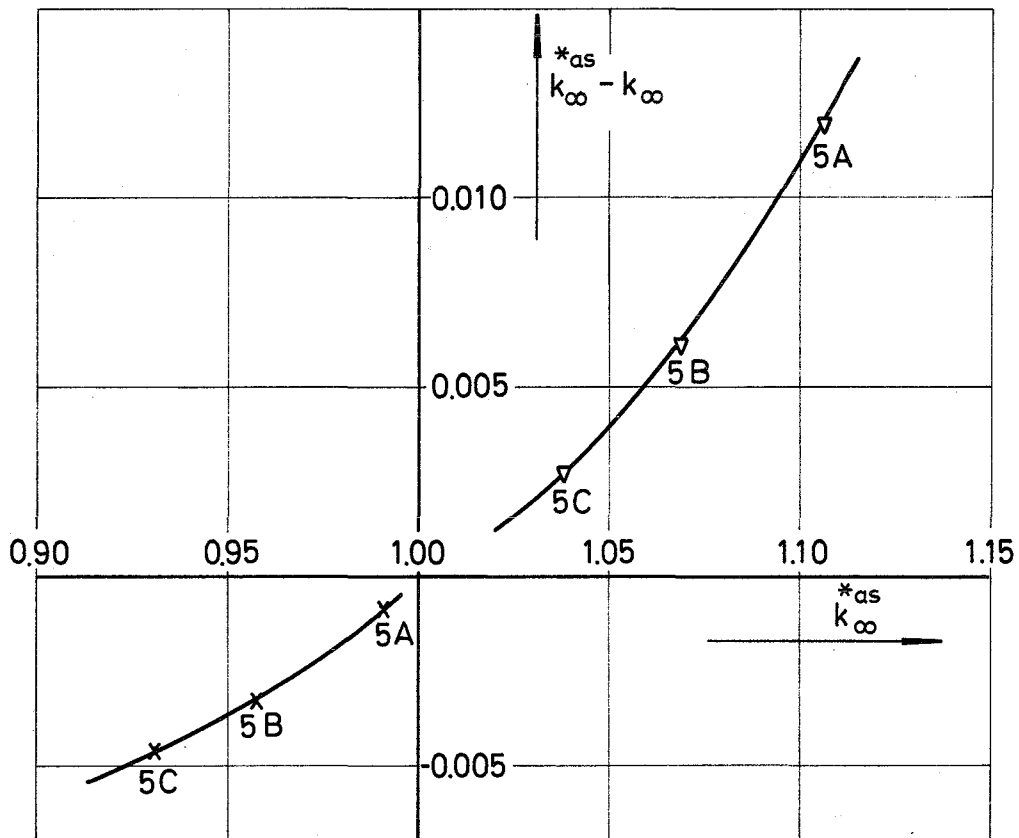


Fig.7 Correction Terms $k_{\infty}^{*as} - k_{\infty}$ for Different Assemblies.

- x Homogeneous calculation with SNEAK set
- \nabla Homogeneous calculation with ABN set

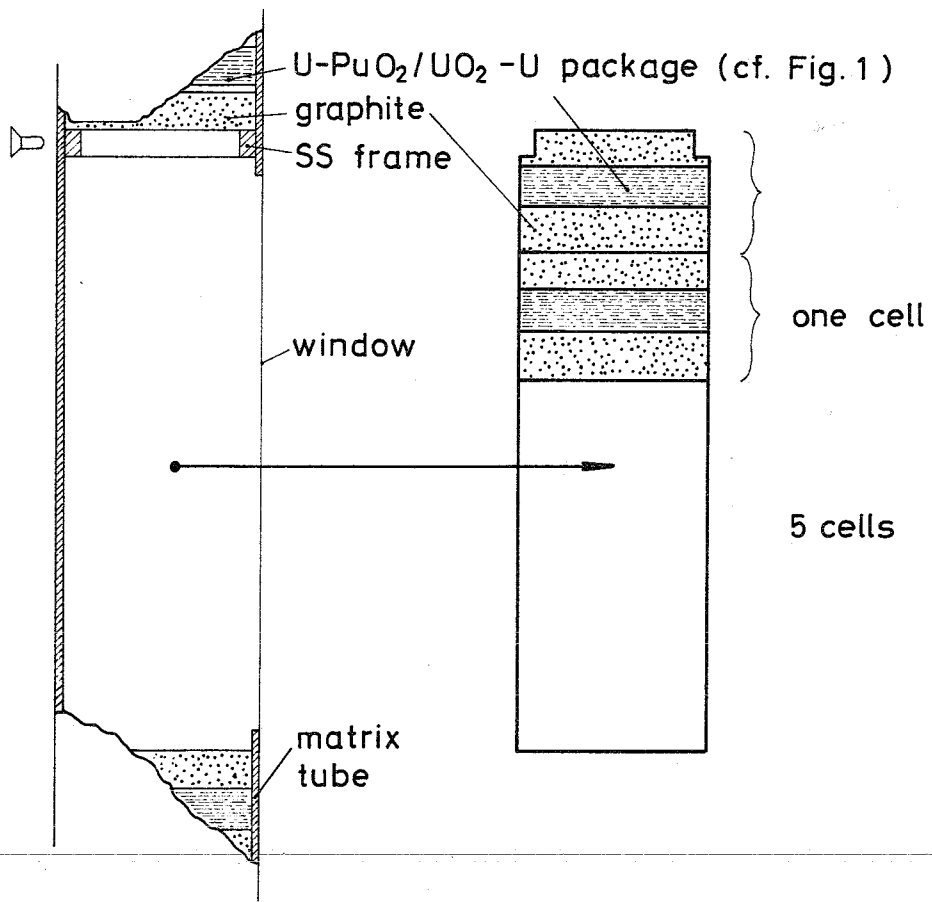


Fig.8 : Arrangement for Cell Replacement Experiments

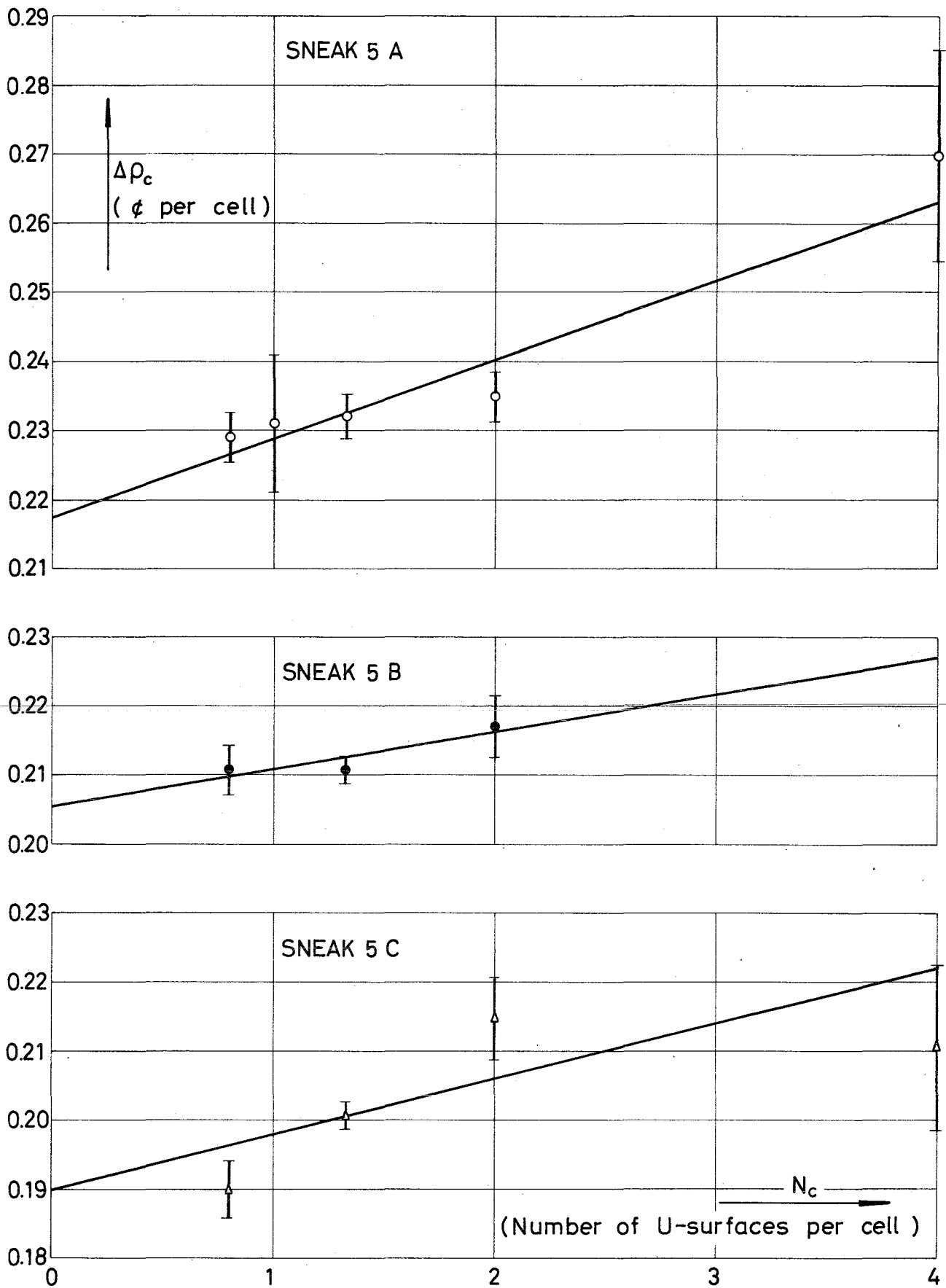


Fig.9 : Results of Cell Replacement Experiments. Reactivity worth of core material per cell versus relative number of uranium surfaces adjacent to void region

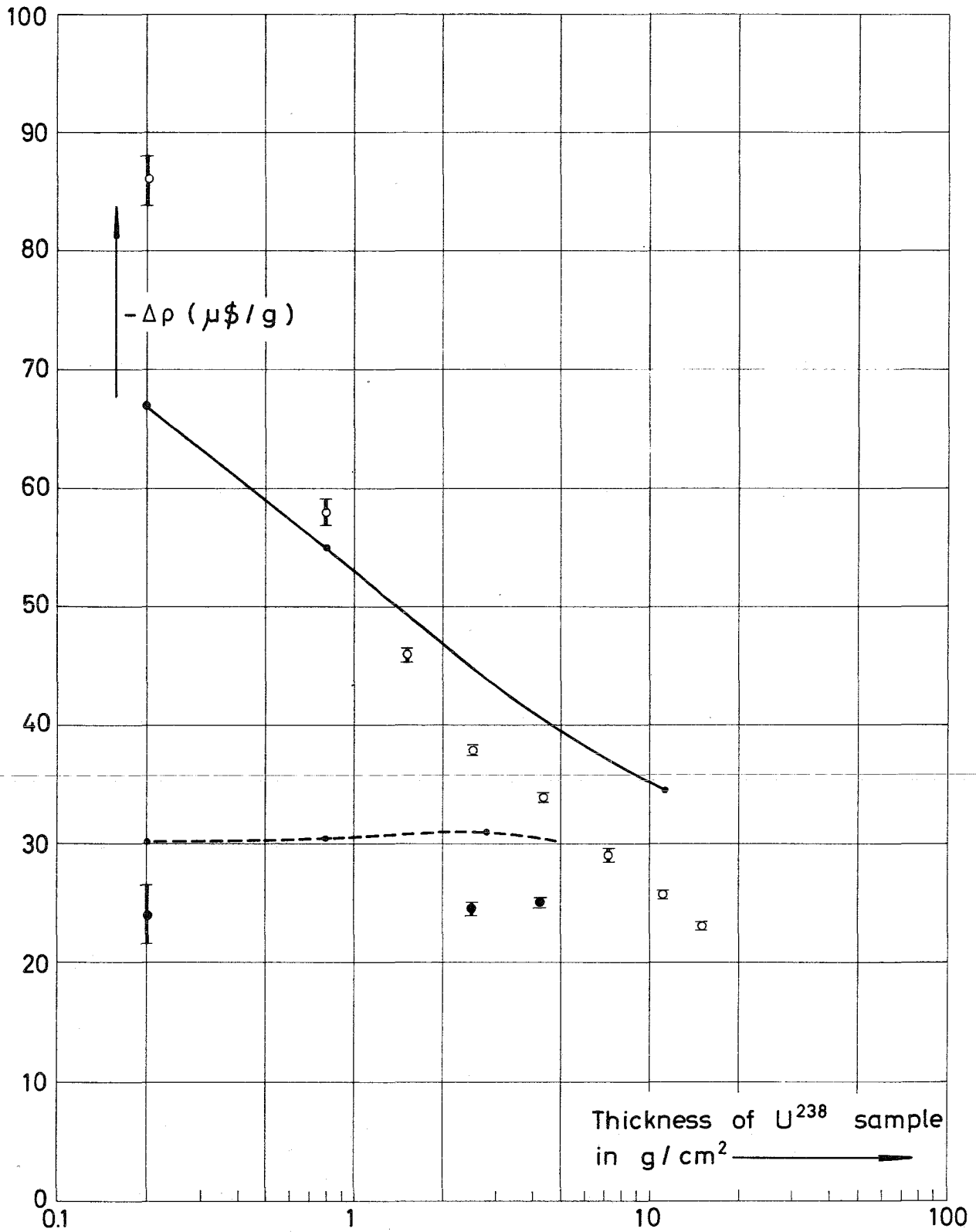


Fig.10: Central Reactivity Worth of U^{238} in SNEAK 5C

 measurement with sample in graphite
 " " " " " U_{nat}
 sample in graphite } heterogeneous perturbation
 sample in U_{nat} } calculation with SNEAK set

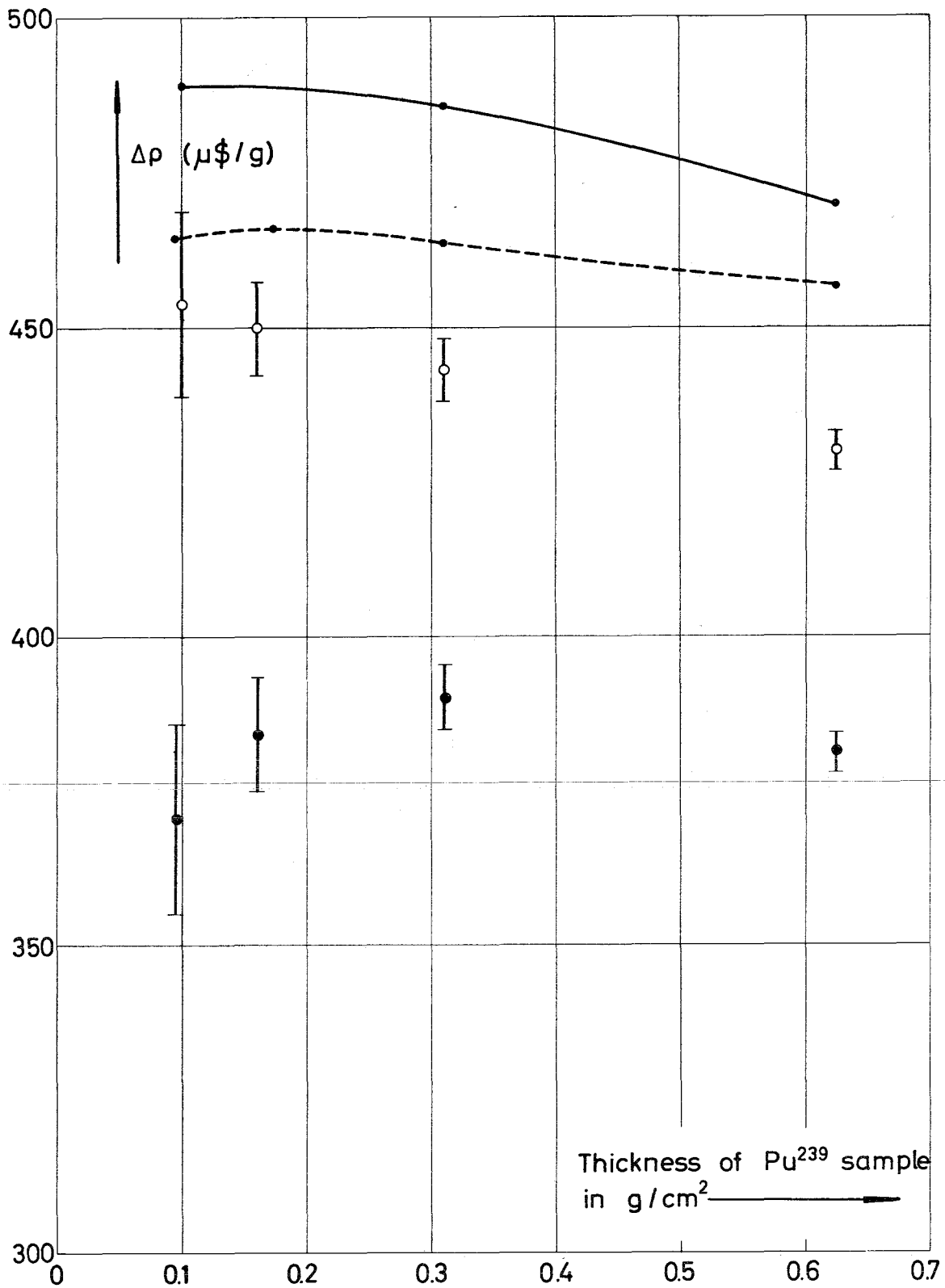


Fig.11: Central Reactivity Worth of Pu^{239} in SNEAK 5C

\circ measurement with sample in graphite
 \bullet " " " " U_{nat}
 — sample in graphite } heterogeneous perturbation
 - - - sample in U_{nat} } calculation with SNEAK set

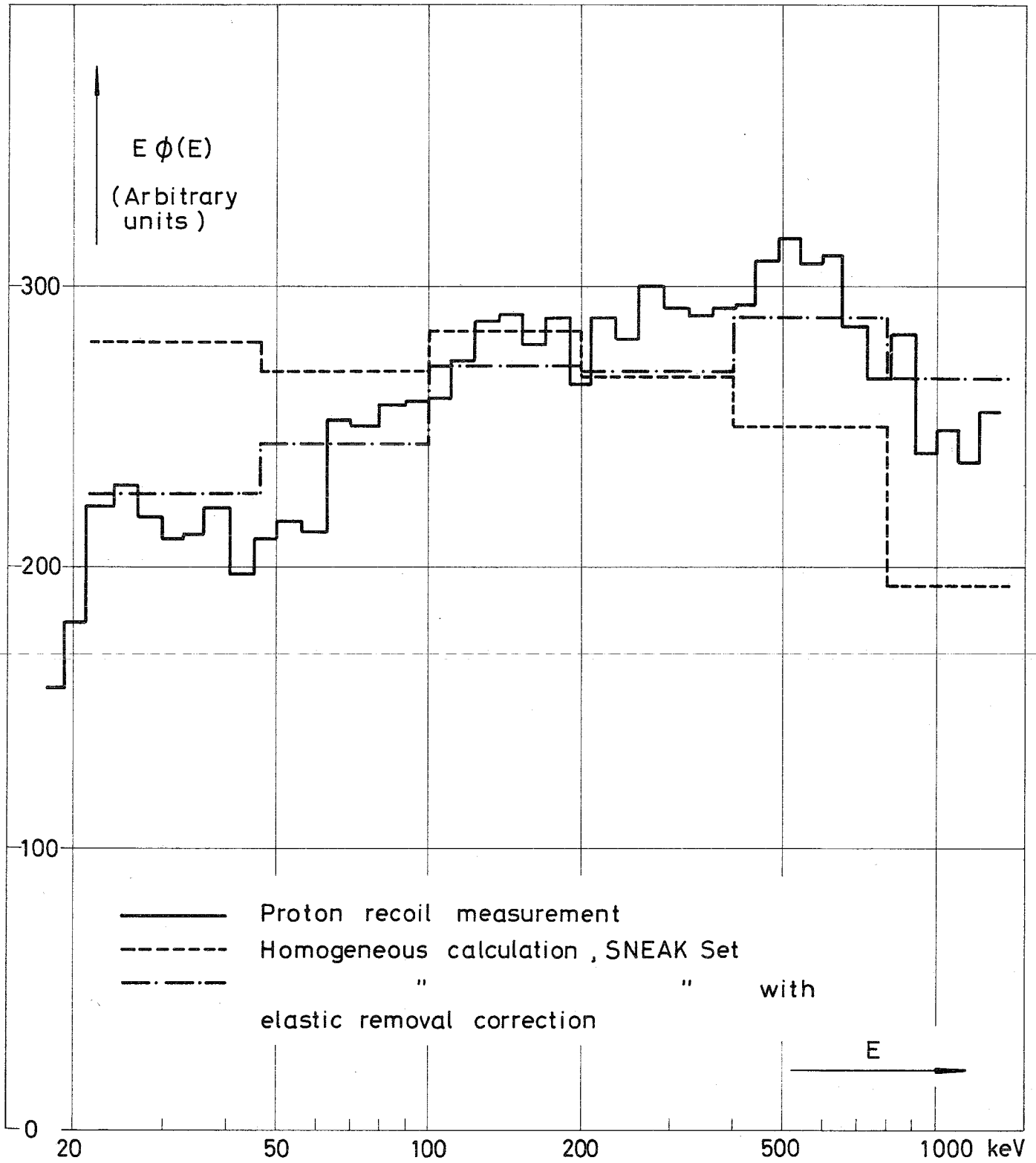


Fig.12 : Proton Recoil Spectrum Measurement at the Centre of SNEAK 5 C

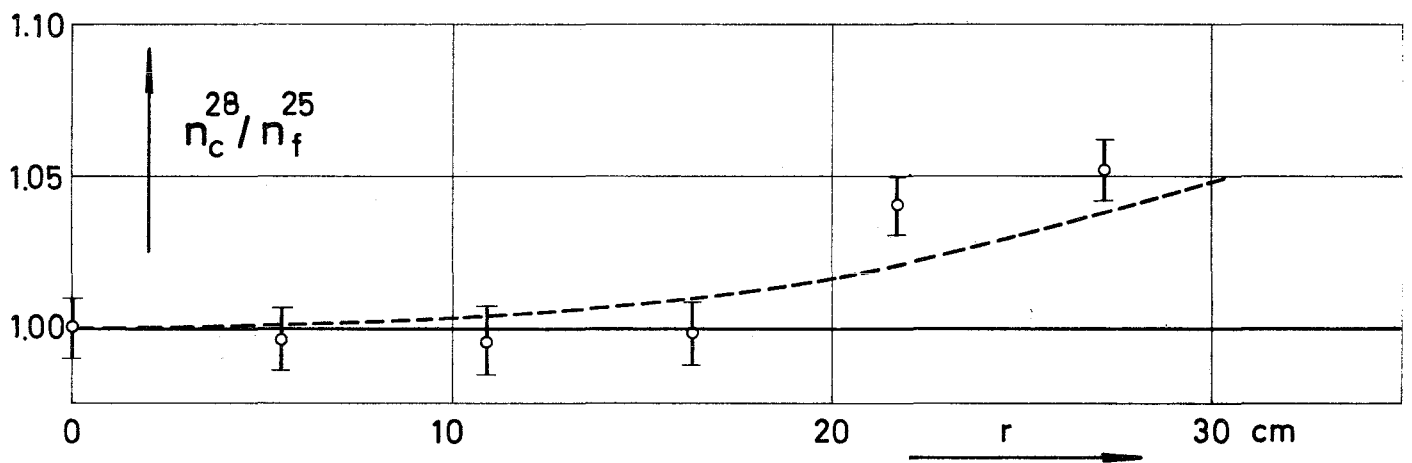
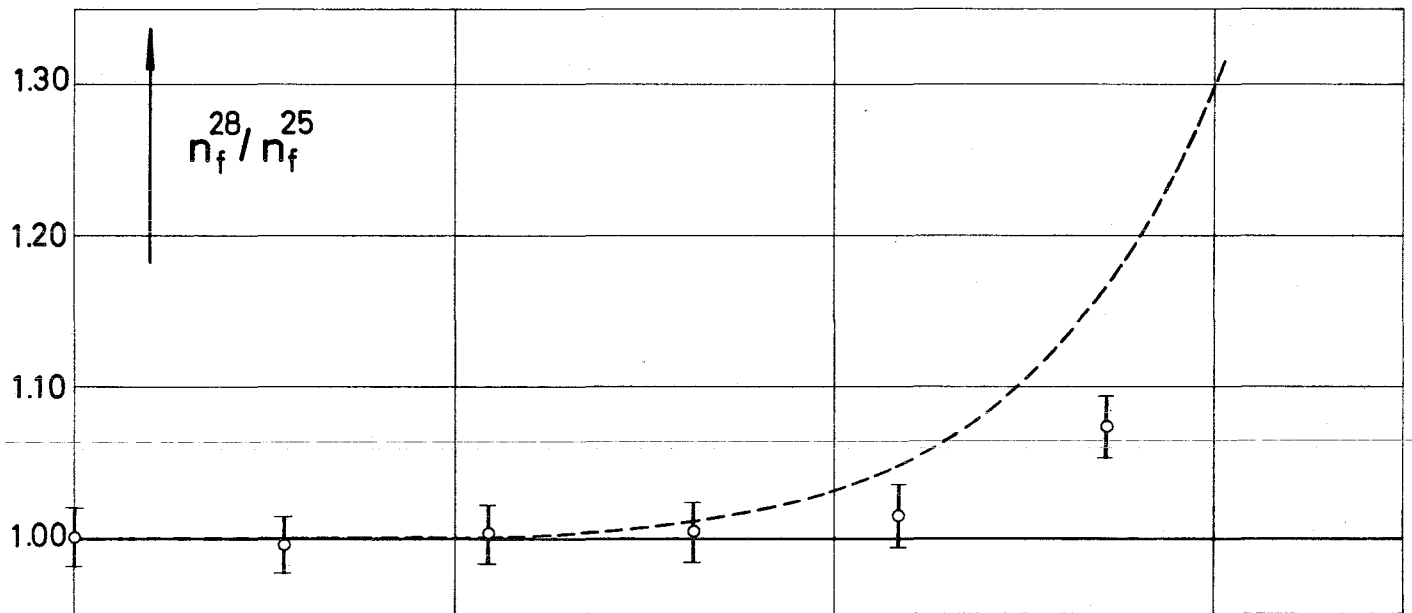
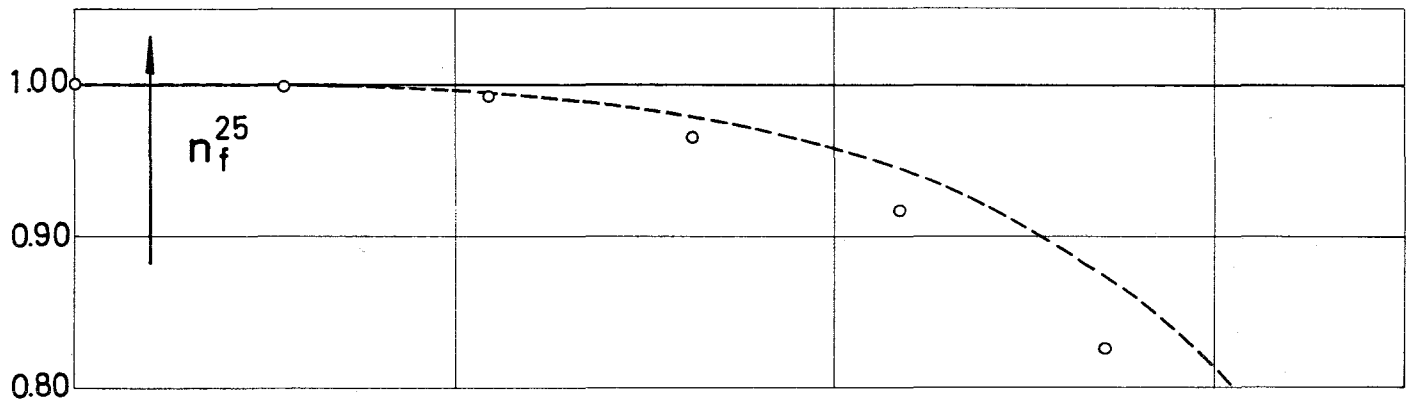


Fig. 13: Radial Reaction Rate Traverses in SNEAK 5C, normalized to 1 at $r=0$

 foil activation measurement
 ----- two-dimensional diffusion calculation (SNEAK set)

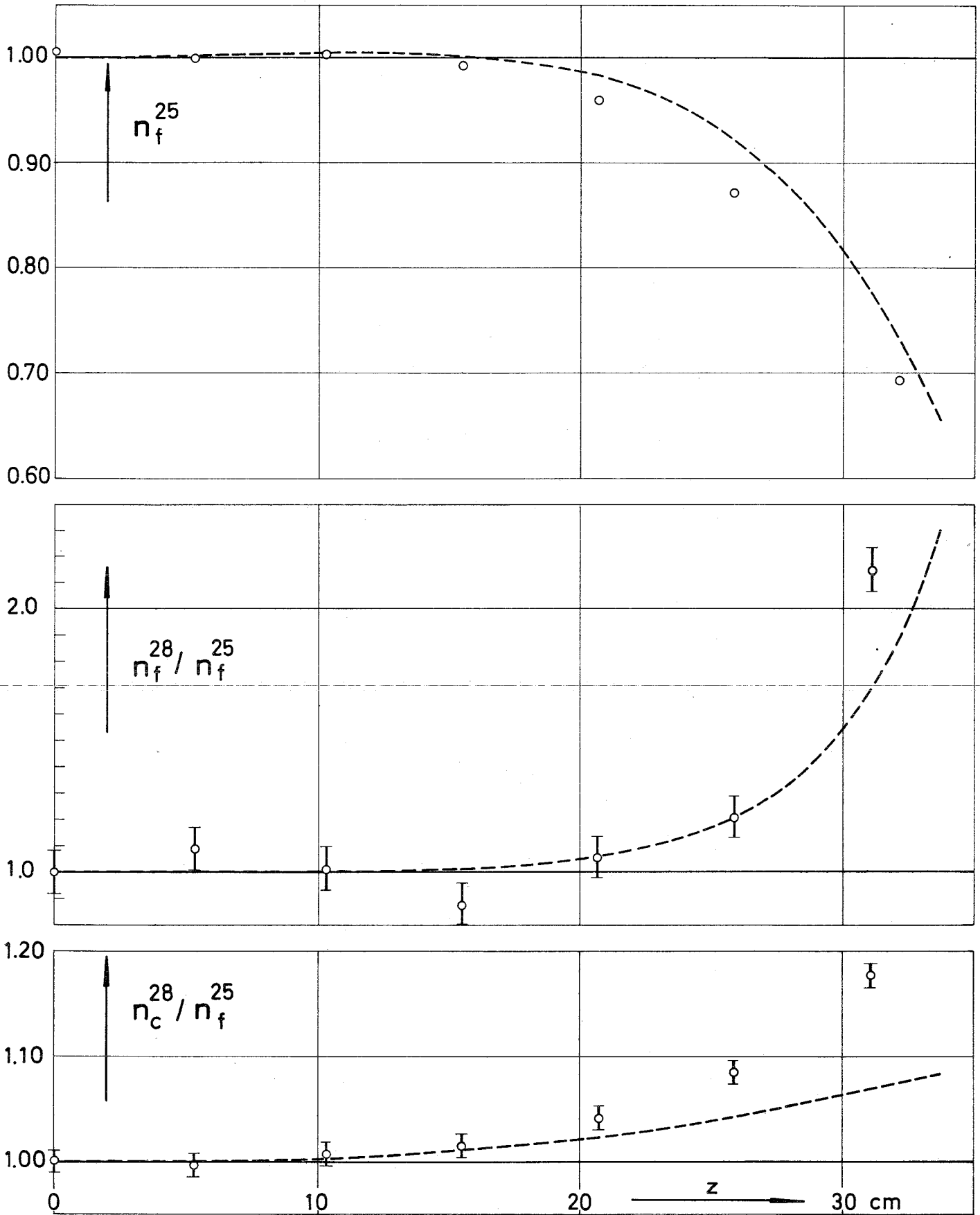


Fig.14 : Axial Reaction Rate Traverses in SNEAK 5C , normalized to 1 at $z=0$

○ foil activation measurement
 ----- two-dimensional diffusion calculation (SNEAK set)

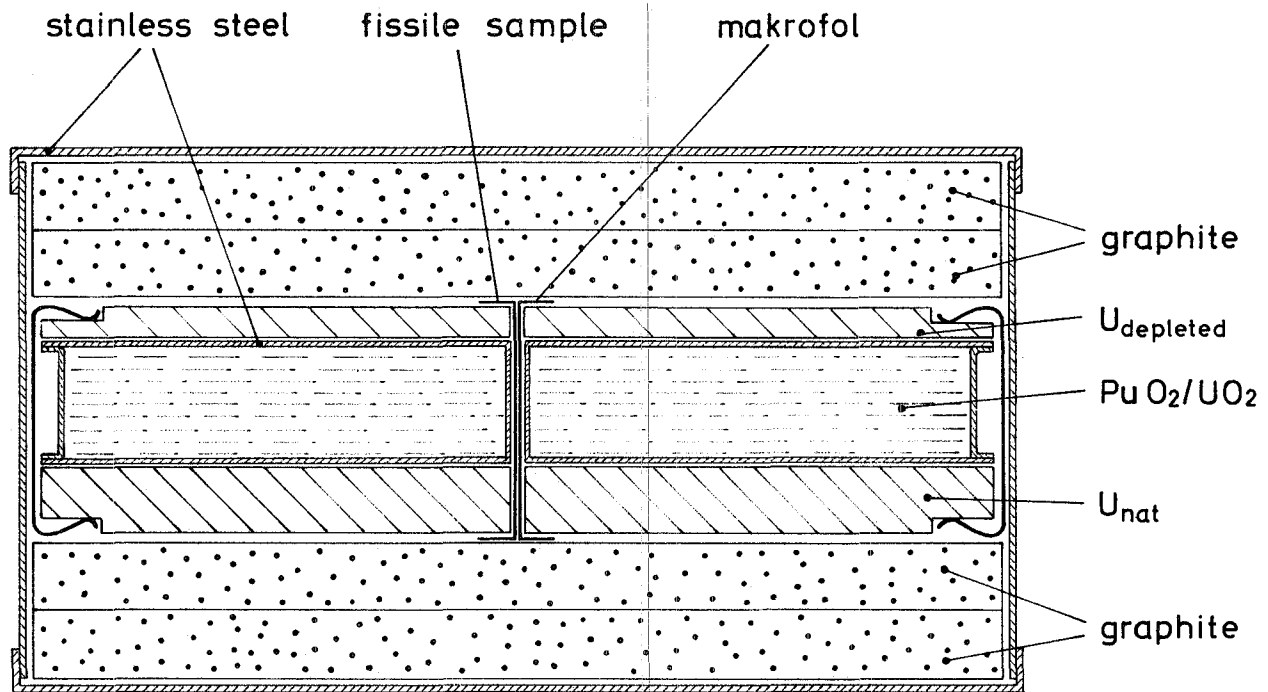


Fig.15 : Equipment for Fine Structure Measurement

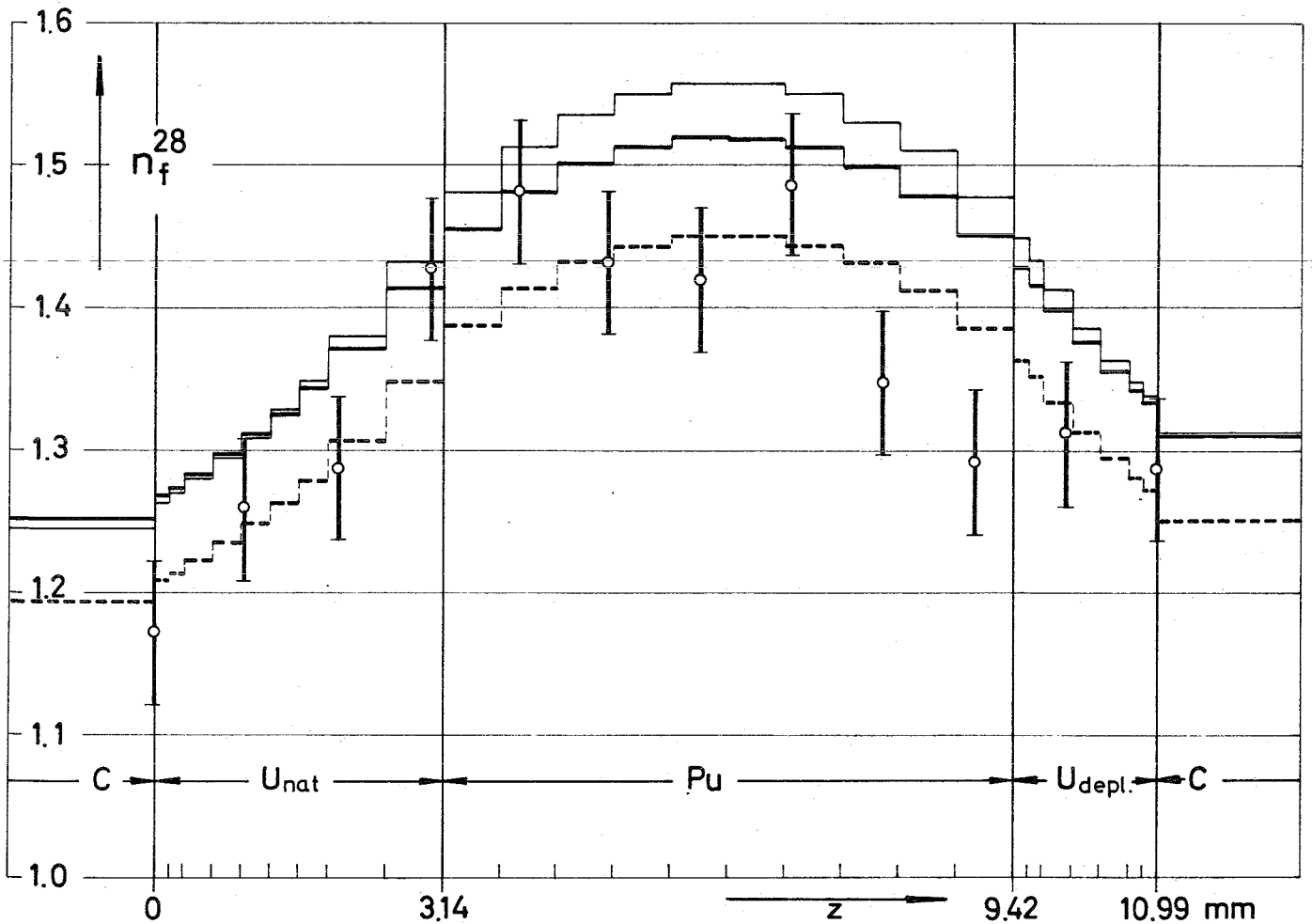
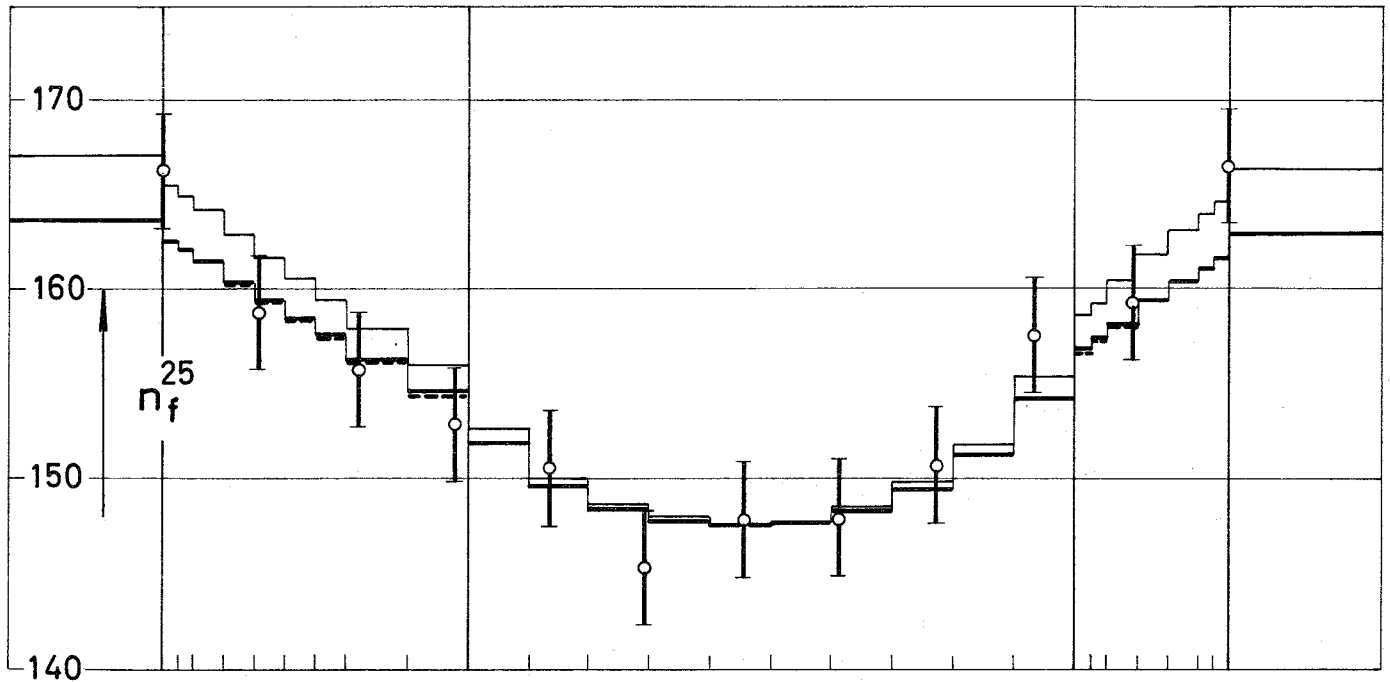


Fig. 16 Fine Structure of Fission Rates in the Central Lattice Cell

- Measurement with SSTR technique; U^{235} data normalized to calculation
- ZERA calculation (SNEAK set) with averaged atom numbers
- - - ZERA calculation (MOXTOT set) with averaged atom numbers
- ZERA calculation (SNEAK set) with actual atom numbers

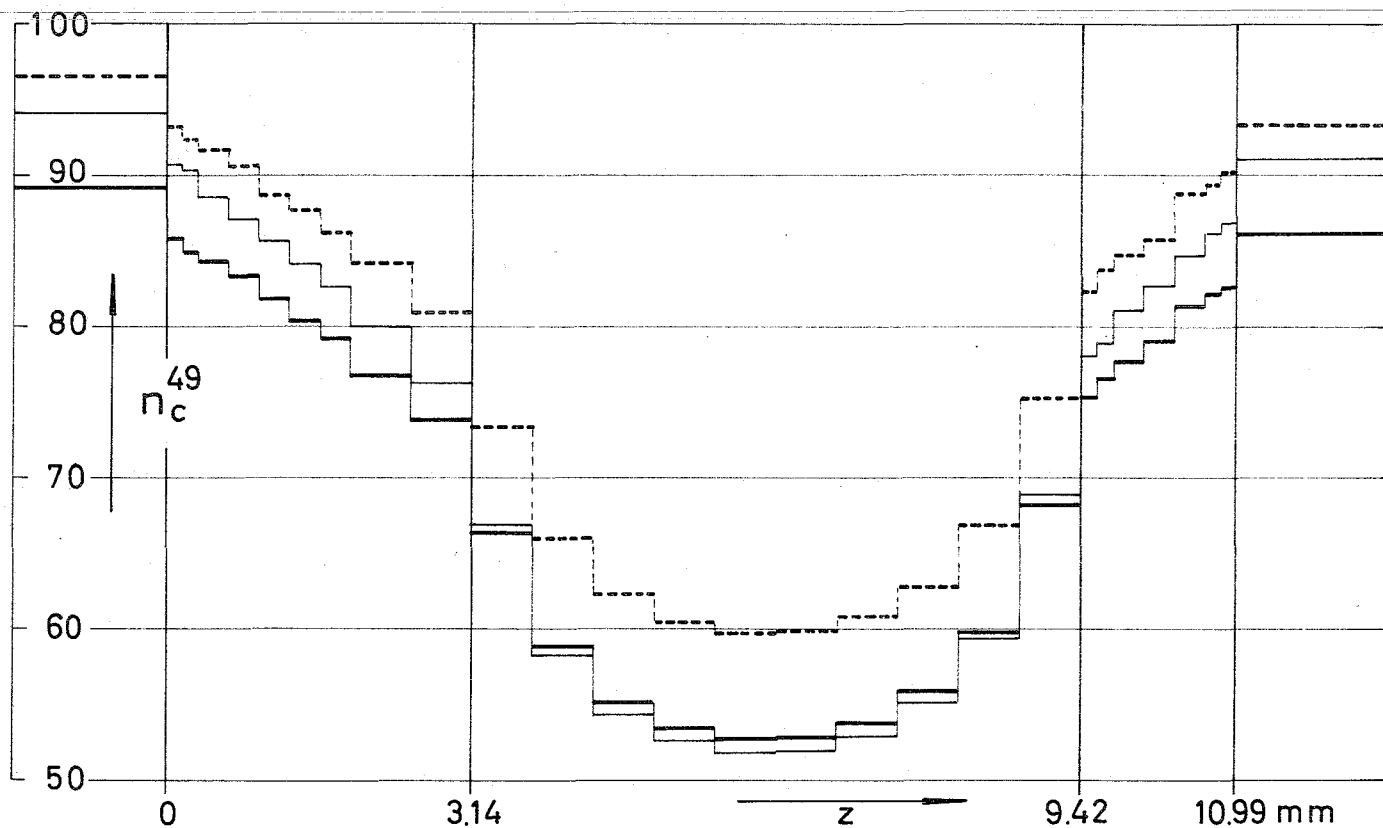
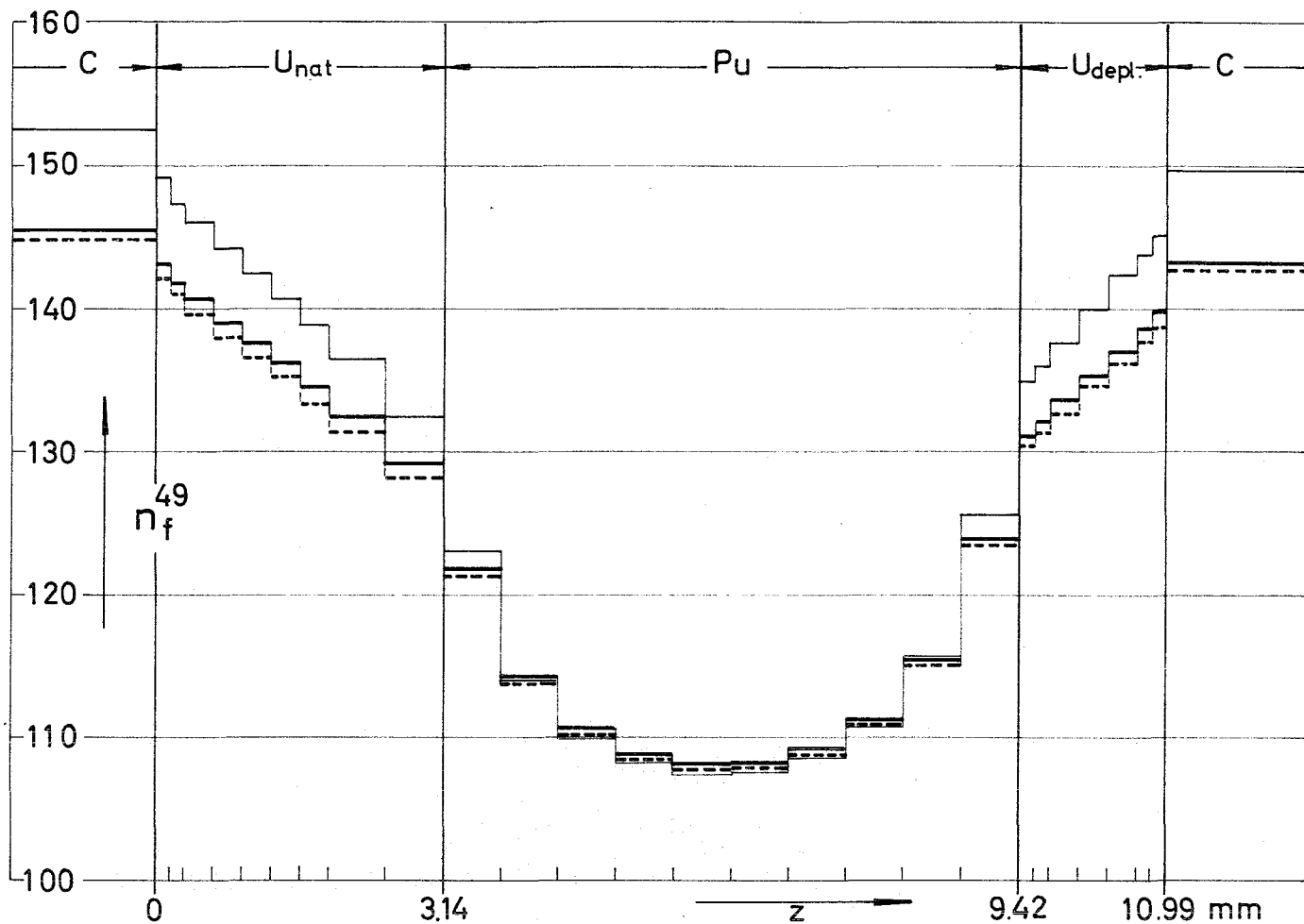


Fig. 17 Fine Structure of Pu^{239} Reaction Rates in the Central Lattice Cell

- ZERA calculation (SNEAK set) with averaged atom numbers
- - - ZERA calculation (MOXTOT set) with averaged atom numbers
- · - ZERA calculation (SNEAK set) with actual atom numbers

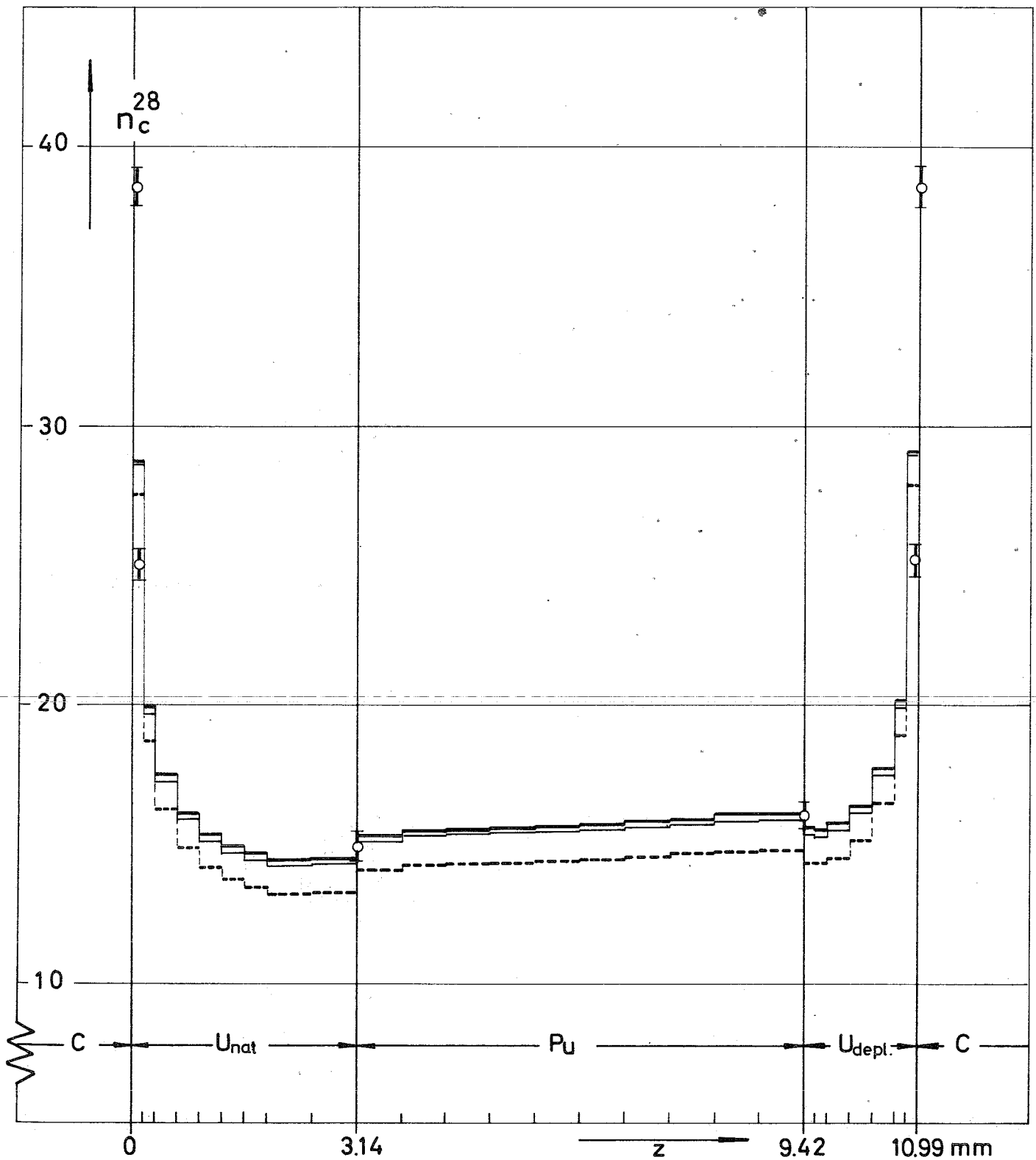


Fig.18 Fine structure of the U^{238} Capture Rate in the Central Lattice Cell

-  Measurement by γ -x-ray counting; U^{235} data in Fig.16 normalized to calculation
-  ZERA calculation (SNEAK set) with averaged atom numbers
-  ZERA calculation (MOXTOT set) with averaged atom numbers
-  ZERA calculation (SNEAK set) with actual atom numbers

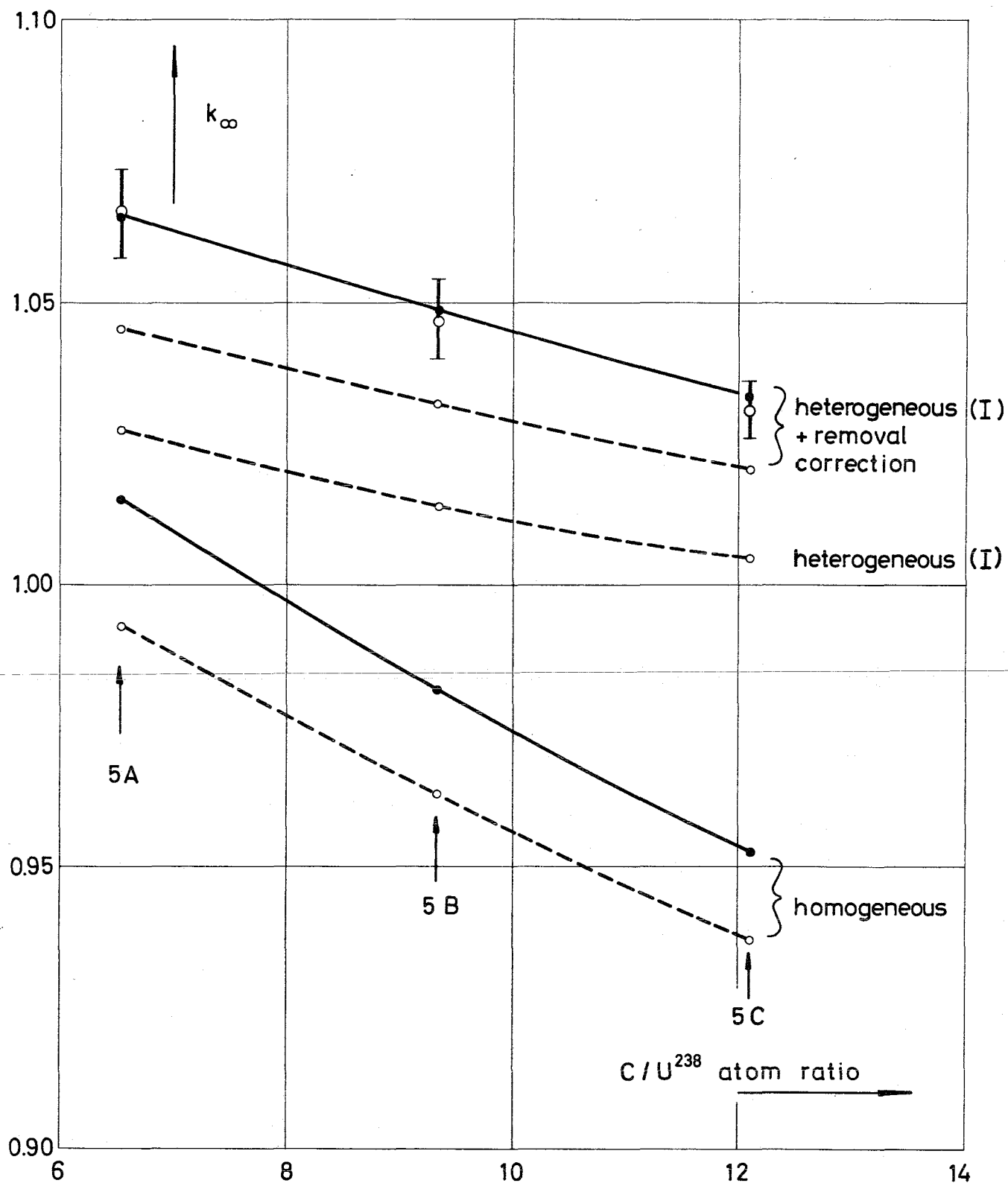


Fig. 19 : k_{∞} of SNEAK 5 as a Function of C/U-Ratio

-  Experiment
-  Calculation with SNEAK set
-  Calculation with modified SNEAK set (MOXTOT)